Delft University of Technology

Thesis small scale equilibria in tidal basins

A data-analysis and case study in the Ameland Inlet

Friday 11^{th} of March 2022

TU Delft Delft University of Technology

Rijkswaterstaat
Ministerie van
Infrastructuur en Waterstaat

Deltares
Enabling Delta Life

Thesis small scale equilibria in tidal basins
A data-analysis and case study in the Ameland Inlet

General information

Writer
Sebastiaan Diepeveen, 4315448

University
Delft University of Technology
Faculty Civil Engineering and Geosciences
Coastal Engineering

Committee
Prof. dr. ir. Zheng Bing Wang
Drs. Quirijn Lodder
Dr. Ymkje Huismans
Dr. ir. Bram van Prooijen

Date
Friday 11^{th} of March 2022

Acknowledgement

I have put a great deal of effort in the work laying in front of you. But it was not possible without the help of a number of people.

First of all I want to thank Prof. dr. ir. Zheng Bing Wang. Not only his sharp questions and critical mindset helped me to step up my game during meetings but also all the papers he has written on the subject have helped me a great deal in the theoretical part of this thesis.

I would like to thank Drs. Quirijn Lodder for his suggestion of using a hydrodynamical model in finding the watersheds but more importantly, checking in on me and making a lot of time available to answer my questions and brainstorm about solutions.

I would like to thank Dr. Ymkje Huismans for her help in the matlab ASMITA modelling and for her accessibility and positivity during the meetings we had.

I would like to thank Dr. ir. Bram van Prooijen for accompaniment of my startup and green light meetings.

I would also like to thank my committee for granting me the opportunity to work from England for a period of time.

Last of all I would like to thank my girlfriend, friends and family for the support I have gotten throughout the period of my thesis.

1 Abstract

The behaviour of tidal basins has been predicted using a modelling approach in which a morphological equilibrium for an entire basin was used frequently in the past. Because tidal basins have, to an certain extend, a fractal nature, it is expected that this approach could be used with a morphological equilibrium for subbasins as well.

In the first part of this thesis the morphological equilibrium for subbasins is examined. A numerical simulation using tracers is conducted in order to find the watersheds of the Ameland Inlet. The watersheds are used to divide the basin into subbasins of different scales. These subbasins are used to find a morphological equilibrium between the channel volume and tidal prism. The applicability limitations of the morphological equilibrium relation are also investigated in this part of the research.

In the second part of the research the newfound equilibrium is applied in an Asmita model. The modelling exercise is done in order to showcase a proof of concept of the multi element modelling approach. In this modelling approach both a 6 and 10-element model are used to look for the spatial differences in morphological behaviour within a basin.

In the first part of this thesis an equilibrium for the channel volume with respect to the tidal prism of subbasins in the Ameland inlet is found. This equation can be applied to basins (Channel and flat combined) with a minimum area of 40 km^2. This limitation is for both the equilibrium study as the Asmita modelling. The modelling exercise proofs that the multi element Asmita modelling is possible and gives a good insight into the spatial differences in morphological behaviour within the Ameland Inlet.

Table of Contents

1 Abstract **3**

2 Introduction **6**
2.1 The long term morphological equilibrium of the Wadden sea . . . 6
Texel and Vlie Inlet . . . 7
Eierlandse Gat Inlet . . . 8
Ameland Inlet . . . 8
Frisian Inlet . . . 8
2.2 Equilibrium relations . . . 8
2.3 Asmita modelling . . . 9
2.4 Research questions . . . 11
2.5 Hypotheses . . . 12

3 Method equilibrium relations **13**
3.1 Chosen Basin . . . 13
3.2 Hydrodynamic & particle simulation . . . 13
3.3 Tidal watersheds & subbasins . . . 15
3.4 Hypsometric curve . . . 17
3.5 Preliminary results . . . 18
3.6 Applicability . . . 19
Constant watersheds . . . 20
Overlap analysis . . . 21
Conclusion . . . 21

4 Results equilibrium study **23**
4.1 Conclusion . . . 23
4.2 Application to other basins . . . 24

5 Method multiple element Asmita modelling **26**
5.1 6 element model . . . 26
5.2 10 element model . . . 29

6 Results multiple element Asmita modelling **33**
6.1 6 element model . . . 33
No sea level rise . . . 33
2 mm sea level rise per year . . . 35
8 mm sea level rise per year . . . 37
6.2 10 element model . . . 39
No sea level rise . . . 39
2 mm sea level rise per year . . . 41
8 mm sea level rise per year . . . 44

7 Discussion **47**

8 Conclusion **49**

9 Recommendations for future work **50**

A 6 element figures 4 and 6 mm/year sea level rise **53**

B 10 element figures 4 and 6 mm/year sea level rise **55**

C 3 element matlab model **57**

D 6 element matlab model **62**

E 10 element matlab model **67**

2 Introduction

This is a thesis about the morphological equilibrium of tidal subbasins conducted and written by Sebastiaan Diepeveen. The research in this thesis can be divided into two main parts. Firstly, the deduction of a morphological equilibrium relation between channels in tidal subbasins and secondly the application of the newfound equilibrium in an Asmita model in order to model the differences in morphological behaviour between different parts of a basin. The remainder of this section consists of the background of long-term morphological equilibria, a description of different tidal basins, the theory about equilibrium relations, an explanation of Asmita modelling and a research proposal.

2.1 The long term morphological equilibrium of the Wadden sea

The Wadden Sea came to exist 7000 years ago. Under the influence of sea level rise, the sea has migrated landwards, up until the middle ages, when the landwards boundaries became fixed because of embankments (Elias et al., 2012). The system of tidal barriers and flats is able to import sediment, to mitigate the drowning of the system under influence of sea level rise. In the past century, closures of the Zuiderzee (1932) and Lauwerszee (1969) have influenced the system further. It had to find a new morphological equilibrium (Kragtwijk et al., 2004). A dataset of the bathymetry of the Wadden sea is available from 1935 to present day. Although the data is very valuable, individual influence of the closures and sea level rise is hard to distinguish in the data. Furthermore the timescale of morphological changes is much longer than the time of the observed data. Predictions of future behaviour of the Wadden Sea can therefore not be based on analysis of the historical changes (Elias et al., 2012) alone, but has to be investigated using morphological models.

A lot of the consequences of sea level rise are well known, but the threat to the flats in a tidal basin may be less top of mind. The sea level rise increases sedimentation rates in the basins, but, as this happens with a delay, some drowning is likely. This self-preserving feature of a system of tidal flats and basins is very valuable, but has its limits. The question rises if the sedimentation rate in the Wadden Sea will be able to keep up with the sea level rise. If this is not the case, partial loss or drowning will occur.

This sedimentation plays a part in a dynamic equilibrium. As tide-residual transport, caused by asymmetry of the tidal wave, induces morphological changes, a system will change its bathymetry, to reduce this asymmetry. At the moment where the asymmetry vanishes, the tide-residual transport disappears and the system is in a morphological equilibrium (Van Goor et al., 2003). As the sea level rises, the Wadden sea does not have a static equilibrium. The equilibrium, which can be reached, is a dynamic equilibrium, in which the system is importing sediment at a rate that is keeping up with sea level rise.

A demand (shortage or surplus) does not necessary lead to corresponding transport. If a demand is satisfied depends on the sediment availability and transport capacity. Two linked systems can have complementary or competitive demand. If both systems encounter a surplus or shortage, the systems are competitive. If one system has a surplus and the other has a shortage, the systems are complementary. (Van Goor et al., 2003).

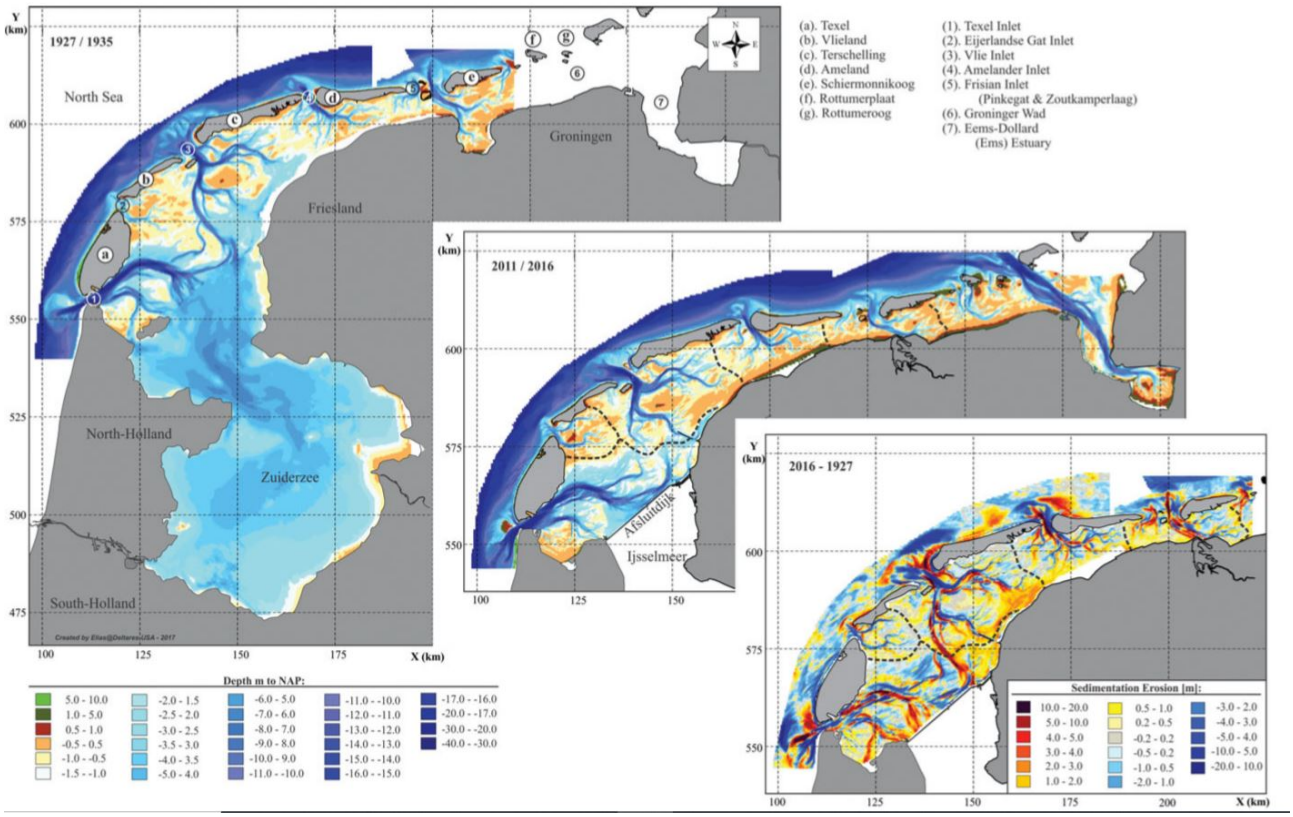

Figure 1: Changes in channels and shoals in the Dutch Wadden Sea over the period 1927–2016. Upper panel: Bathymetry representative for the 1927–1935 time frame (prior to closure of the Zuiderzee). Middle panel: Recent bathymetry based on surveys over the years 2011–2016. Lower panel: Sedimentation–erosion pattern over the interval 1927–2016. (Wang et al., 2018)

The different basins in the Wadden sea are in a different state with respect to their morphological equilibrium. As said the closures of the Zuiderzee (1932) and the Lauwerszee (1969) still have their impact on the Texel and Vlie Inlets (Zuiderzee) and the Frisian Inlet (Lauwerszee). The current state of the inlets is described below.

Texel and Vlie Inlet

These inlets are mainly influenced by the closure of the Zuiderzee in 1932. The area of these basins was reduced by the Afsluitdijk from over 4000 km^2 to 1400 km^2 (Elias et al., 2012). The closure of the Zuiderzee decreased the area of these basins, but the influence on the tidal prism is very limited, it increased a little bit. Because of this, the channels in this system only experienced limited sedimentation, while in the shallow parts sedimentation was more substantial (Wang et al., 2018). In these basins, the tide changed from a progressive, to a standing wave. Furthermore, the hard structure of the Afsluitdijk increased the tidal range from 1.1 to 1.4 m at Den Helder (Elias et al., 2003). These inlets together imported over $450 \cdot 10^6$ m^3 of sediment (Elias et al., 2012). $300 \cdot 10^6$ m^3 was imported through the Texel Inlet. $130 \cdot 10^6$ m^3 came from the ebb-tidal delta, with the remaining part being eroded from adjacent coasts (Elias et al., 2003). From 1935 the erosion rate of the Vlie ebb-tidal delta (2 million m^3/y) is relatively small with respect to the sedimentation rate in its tidal basin (3 million m^3/y). It is likely that sediment in this system is imported from the Texel Inlet system. These two basins are a sediment-sharing system (Elias et al., 2012). The Texel and Vlie Inlets have

high sedimentation rates (4.69 mm/y) compared to the other basins in the Wadden sea system, coming from the large scale interventions in the past (Wang et al., 2018). The erosion of the ebb tidal delta of the Texel system has decreased over the past decades, this has partly to do with nourishments in the system, but cannot entirely be explained by this (Elias and van der Spek, 2017).

Eierlandse Gat Inlet

The Eierlandse Gat Inlet is the smallest system of the Dutch Wadden sea. It has a surface area of 153 km^2. The system erodes 2.9 mm per year since 1935, probably caused by the hydraulic changes caused by the closure of the Zuiderzee in 1935. It is the only basin in the Dutch Wadden sea dealing with erosion (Elias et al., 2012). The ebb tidal delta is growing (Elias, 2019).

Ameland Inlet

This system has no influence of major closures in the Wadden sea. It is assumed to be in dynamic equilibrium (Wang et al., 2018). As the influence of a closure is absent, the influence of sea level rise can be seen quite well in this basin. The basin had a sediment import of 1.04 million m^3/y in the period 1926-2015 and 1.43 m^3/y in the period 1989-2015 (Elias, 2019). The increase in sedimentation can suggest a changing dynamic equilibrium, caused by sea level rise, although the possibility that increasing sedimentation in the basin is caused by an increase in nourishments in the Ameland shoreface, should be taken into consideration (Wang et al., 2018).

Frisian Inlet

The Frisian Inlet has two main inlet channels, Pinkegat and Zoutkamperlaag. Together they form the Frisian Inlet and have a common ebb-tidal delta. Before the closure of the Lauwerszee, both channels had a cycle between a single and double channel configuration. (Elias et al., 2012). In contrast to the Zuiderzee closure, the closure of the Lauwerszee caused a large reduction in tidal prism, from 306 m^3 to 200 m^3 (Elias et al., 2012). Because of this difference the channels of the Frisian Inlet were too big for the morphological system. Whereas the channels of the Texel and Vlie Inlets didn't reduce in size and sedimentation was mostly on the tidal flats, in the Frisian Inlet sedimentation was visible over the entire system, also reducing the size of the channels (Wang et al., 2018). The Frisian Inlet shows the fastest sedimentation rates, with 6.66 mm/y (Wang et al., 2018). This sedimentation is largest in the Zoutkamperlaag. Recently some erosion is taking place in the Pinkegat (Elias, 2019). This sedimentation predominantly took place at the closed-off channel towards the Lauwerszee. The channel extended along the closure dam, causing the tidal divide to move a few km to the east (Oost, 1995). The last few decades sedimentation is back at its pre-closure rate. This indicates that the inlet is getting closer to its morphologic equilibrium again (Elias et al., 2012).

2.2 Equilibrium relations

Equilibrium relations are an important part of this thesis. One of Eysinks papers has a comprehensive summary on the different morphological equilibrium relations. In this paper he described the findings of several other studies (Eysink, 1991). First of all the relationship between the tidal prism (P) and the channel volume below MLW (V_C) is described:

$$V_C = \alpha_C \cdot P^{1.55} \tag{1}$$

Also the volume of the ebb-tidal delta (V_O) can be correlated to the tidal prism (Eysink, 1991):

$$V_O = \alpha_O \cdot P^{1.23} \tag{2}$$

In a paper published later, Eysink described the correlation between the basin area (A_b) and the area of the tidal flats (Eysink, 1992):

$$\frac{A_{fe}}{A_b} = 1 - 2.5 \cdot 10^{-5} \cdot A_b^{0.5} \tag{3}$$

This combined with the equilibrium height of a tidal flat (h_{fe}) can be combined to a tidal flat volume:

$$\begin{aligned} h_{fe} &= \alpha_{fe} \cdot H \\ V_{fe} &= A_{fe} \cdot h_{fe} \end{aligned} \tag{4}$$

The parameters in the morphological equilibrium relations are the following (Wang et al., 2018):

$$\begin{aligned} \alpha_C &= 1.02 \cdot 10^{-5} \\ \alpha_O &= 2.92 \cdot 10^{-3} \\ \alpha_{fe} &= 0.34 \end{aligned} \tag{5}$$

2.3 Asmita modelling

Research of the response of entire basins of the Wadden sea using Asmita has been done quite some times in the past (Lodder et al., 2019; Stive and Wang, 2003; Van Goor et al., 2003; Wang et al., 2018). These studies have been done with a small number of elements, usually one or three. In the case of a three element model, the system is schematized with the elements:

- The ebb-tidal delta
- The intertidal flat area
- The total channel volume in the tidal basin
- The adjacent coastal stretches, which serve as outside world boundary

(Van Goor et al., 2003)

This is visualised in figure 2. In case of the one element model, the outside world acts as boundary condition, and the channels are the element used (Van Goor et al., 2003). This is visible in figure 3.

An important hypothesis for the modelling is that the equilibrium relations stated above are valid for each element in the model. The equilibrium volume of the different elements (V_e), is correlated to the tidal range (H), the tidal prims (P) and the basin area (A_b) (Van Goor et al., 2003) and (Eysink, 1991):

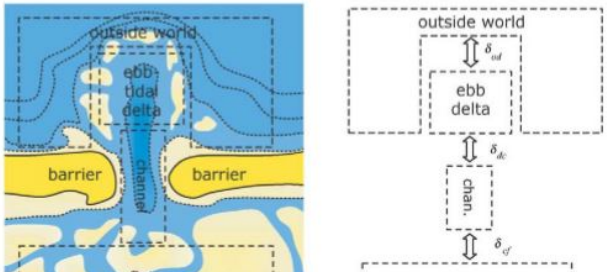

Figure 2: Three element ASMITA model (Van Goor et al., 2003)

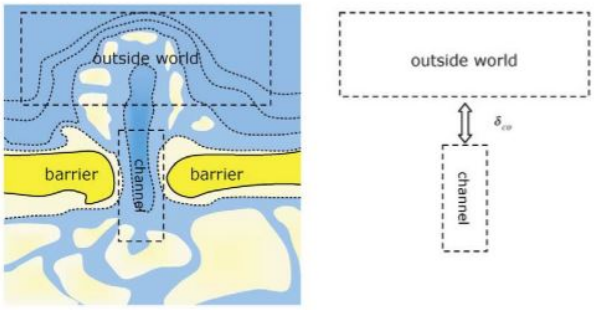

Figure 3: One element ASMITA model (Van Goor et al., 2003)

$$V_e = f(P, H, A_b) \tag{6}$$

The model is based on the conservation of sediment between one element and its neighbours. If sedimentation or erosion takes place in an element, this causes an exchange of sediment of this element with its neighbours. Once a morphological equilibrium is reached, the concentration in each element of the model is equal to the equilibrium concentration. The concentration at this seaward boundary is thus the global equilibrium concentration (c_E) (Van Goor et al., 2003).

The availability of sediment within an element, is the local concentration c_n. The local sediment concentration within an element is noted as c_{ne}. The local demand depends on the local equilibrium concentration and the local concentration $c_{ne} - c_e$. the exchange between two adjacent elements n and m is controlled by the difference $c_n - c_m$. The sediment balance for n becomes:

$$\sum_m \delta_{mn}(c_n - c_m) = A_n w_s (c_{ne} - c_e) \tag{7}$$

The diffusive sediment exchange summed over all adjacent elements (m) to n is represented by the left hand side. The right hand side stands for the local erosion or sedimentation, taking place at the rate w_s. The change in volume is defined as follows:

$$\frac{dV_n}{dt} = \mu_n A_n w_s (c_{ne} - c_e) \tag{8}$$

The value for μ_n is 1 or -1 dependent on the definition of the volume V_n. In case of wet volume it is +1 and in the case of the dry volume it is -1 (Van Goor et al., 2003).

The local and global equilibrium concentration (c_{ne} and c_E) are equal if a system is in morphological equilibrium. If not in equilibrium, the local equilibrium concentration can be calculated using the following relation:

$$c_{ne} = c_E \left(\frac{V_{ne}}{V_n} \right)^{\mu_n r} \tag{9}$$

in which V_ne is the volume the element would have in equilibrium. The term r is usually taken as 2, corresponding to a third power for sediment transport as a function of the mean flow (Van Goor et al., 2003).

An important forcing of a dynamic equilibrium is sea level rise. The rate of volume change caused by sea level rise can be written down in the following way:

$$\frac{dV_{SLR}}{dt} = \mu_n A_n \frac{d\zeta}{dt} \tag{10}$$

in which $d\zeta/dt$ is the rate of the sea level rise. This expression can be put into equation 2.3:

$$\frac{dV_n}{dt} = \mu_n \left(A_n w_s (c_{ne} - c_e) + A_n \frac{d\zeta}{dt} \right) \tag{11}$$

The goal of this study is to investigate the effects of sea level rise on different parts of a Wadden sea basin. An Asmita model with more elements can be made. The difference in morphological response of different parts of a basin can be investigated in this way.

2.4 Research questions

Although the current model is a very useful tool for the study of long-term morphological behaviour of tidal basins, it is quite course. The tho elements in most of the current Asmita models can make a distinction between the behaviour of channels and the intertidal flats, but differences between different channels or flats remain unknown. As a tidal basin has a fractal geometry (Cleveringa and Oost, 1999) and the entire basin behaves along a morphological equilibrium as described in subsection 2.2, it is expected that the channels in subbasins also behave according to a morphological equilibrium relation. In order to build a morphological model that makes a prognosis of the behaviour of tidal subbasins, this morphological equilibrium for tidal subbasins should be known. This thesis thus consists of two major parts, firstly the determination of the morphological equilibrium relation for channels in a subbasin of a tidal basin and secondly applying this equilibrium relation in an Asmita model in order to make a prognosis of different channels and flats within a tidal basin. The following questions act as guideline through the research:

1. Are similar equilibrium relations as the ones described by Eysink (Eysink, 1991) valid if a basin is subdivided into different elements?

2. Is subdividing an ASMITA model a suitable way to describe the spatial differences in response to a disturbance of the morphological equilibrium or the response to a dynamic equilibrium.
3. What are the advantages and disadvantages of subdividing a basin in a model compared to a model which is not subdivided?
4. What are the spatial differences in the response of a basin to a disturbance of its equilibrium or a dynamic equilibrium?
5. How sensitive is a subdivided model to its level of detail?

2.5 Hypotheses

As this thesis has two major parts, it also has two major hypotheses. The first hypothesis is about the morphological equilibrium. Because intertidal basins can be described using an equilibrium as described in 2.2 and a tidal basin has a fractal geometry (Cleveringa and Oost, 1999), there are strong signs that some sort of equilibrium relationship should be able to describe the volumes present in a tidal subbasin, as is the case for a tidal basin.

The second hypothesis regards the subject of the Asmita modelling. Under the assumption that there is a distinct morphological equilibrium as described in the first part of this hypotheses, the second hypothesis is that this equilibrium can be used in order to investigate spatial differences in morphological behaviour within a tidal basin.

3 Method equilibrium relations

In this chapter the manner in which the morphological equilibrium relations were found is described. In order to find small scale equilibria, first subdivisions within a tidal basin should be made. To make subdivisions, the tidal watersheds and bifurcations within a basin should be identified. A subbasin of the tidal basin begins after a bifurcation and stretches until the watersheds at the edges of the intertidal flats. Identifying the bifurcations on a bathymetry map of a basin is quite easy, the watersheds, however, are a lot harder to find. The intertidal flats are situated over a widespread high lying area, without a distinct topographic feature that identifies the watershed. Delft3D is used, in order to identify these tidal watersheds. Using the tidal watersheds different subbasins can be found within the basin. Once the subbasins are identified, the hypsometric curves can be made in order to identify the volumes associated with the tidal prism and the channel volume. These volumes are used to find preliminary results and their applicability in this section. The definitive results are described in section 4.

3.1 Chosen Basin

The research of equilibrium relations in tidal basins in the Waddensea is done in the entire basin of the Ameland Inlet. This basin is chosen because it is one of the few tidal basins that should be close to its dynamical morphological equilibrium (Wang et al., 2018). Due to the closure of the *Zuiderzee* by the construction of the *Afsluitdijk* the areas of the *Marsdiep* and *Vliestroom* inlet systems were reduced massively, while the impact on the tidal prism was limited. Because of this the flats in this system encountered large sedimentation, while the impact on the channels was relatively small. These inlets are thus not in their morphological equilibrium. The *Eierlandse Gat Inlet* is bordered by both of these systems. The closure of the *Zuiderzee* has a small but distinct influence on the (dynamic) equilibrium in this inlet. The total area of this basin increased (Wang et al., 2011), creating a larger tidal prism. The basin has encountered erosion over the past decades (Elias et al., 2012). The closure of the *Lauwerszee* reduced the area and tidal prism in the *Frisian Inlet*. Because of the closure the volume of the channels in this inlet was bigger than the equilibrium volume according to the morphological equilibrium (Wang et al., 2018). Also, the flat volume was too small. Because it being one of the few basins that did not encounter a closure of some sort, the *Ameland Inlet* is one of the few tidal basins that is close to its equilibrium. The other systems that are morphologically unchanged are the smaller systems in the eastern part of the Wadden Sea. Because of their smaller size, one could doubt that these systems are representative of the larger systems in the Wadden Sea. Therefore, the calibration of the morphological equilibrium relations is done in the *Ameland Inlet*.

3.2 Hydrodynamic & particle simulation

In order to find the locations of the different watersheds within the Ameland Inlet, a particle simulation of the entire basin is done. For the particle simulation the computational hydrodynamic model Delft3D is used combined with its particle track plugin Delft3D-Part. This is a so-called offline particle simulation. It is a very fast way of simulating particle motion. The influence of the added particles on the hydrodynamics is not included. This module is not able to incorporate the influence of the particles on the movement of water, because the hydrodynamic simulation is done first and communication files are used to calculate the tracer movement. This method is the "offline" approach. Because we want to monitor the movement of water

by adding virtual tracers, this is very suitable for our situation, even though the influence of individual tracers on the density and movement of water would have been negligible anyway.

In the Wadsea 2009 model the bathymetry of the Ameland Inlet and adjacent inlet systems of three different years are used, 2005, 2011 and 2017. First a hydrodynamic simulation of the entire Wadden Sea is done with the bathymetry of one of the years of interest. The communication files of this simulation are used for the particle simulation. In this particle simulation a total of 4526 particles are released in a regular grid in the Ameland Inlet. The grid lays in between the RD x coordinates 154000 and 193000 and y coordinates 590000 and 609000 with one particle release every 350 m. The particles are released during ebb, just after high tide, to visualise the path that a water body uses to exit the basin from a certain location in the basin. The combined particle tracks of all the locations during several hours while the water in the basin is lowering, give a visualisation of the different subbasins in the Ameland Inlet.

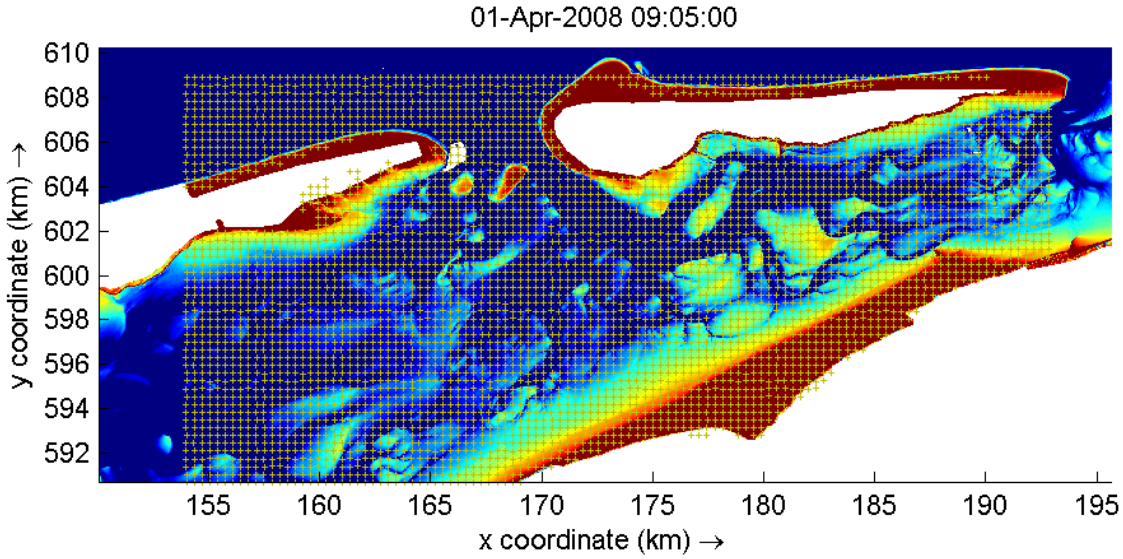

Figure 4: Start grid of particle release locations in the Ameland Inlet

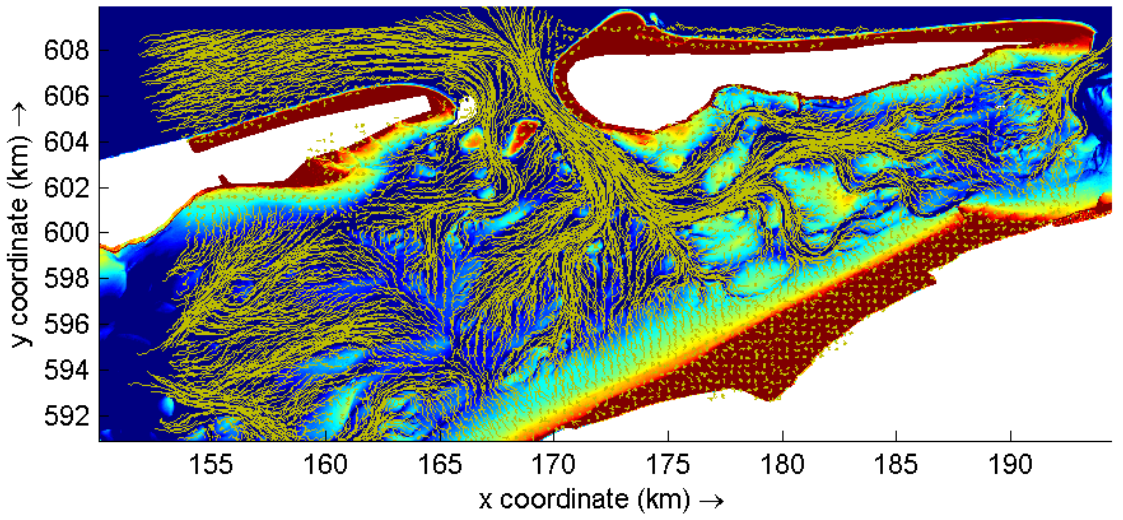

Figure 5: The particle tracks during several hours in the Ameland Inlet

3.3 Tidal watersheds & subbasins

By importing the particles into QGIS via the Python plugin for the software and combining the information with the corresponding bathymetry, clear distinctions between different subbasin become visible. The tidal watersheds of subbasins are drawn by hand in QGIS, using the distinctions between different areas of the particle tracks and the bathymetry of the basin. At the locations where two released particles flow a different direction and use a different channel to exit the basin the tidal watershed is visible. This is combined with the bathymetry of the location in order to choose the most suitable and therefore probable location of the watershed. At some locations the tidal watershed is easier to identify than at other locations. These tools are very useful in deciding the locations of the different tidal watersheds, but in the end, it is impossible to exclude a little bit of personal interpretation to the data. The watersheds are therefore a bit arbitrary, but it is an improvement on how watersheds are usually derived. A few examples of this process are in figure 6.

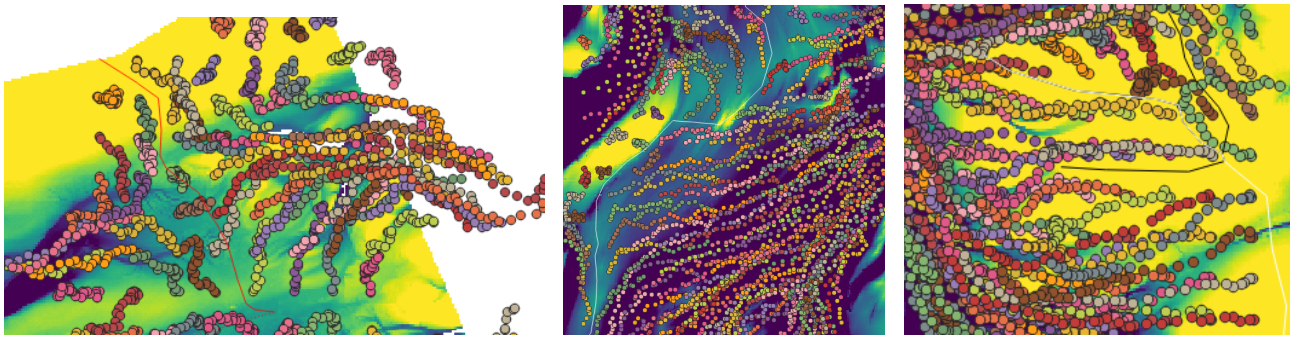

Figure 6: Examples of the determination of the tidal watersheds by using the particle tracks combined with the bathymetry

In the three examples of figure 6 there are a lot of cases where the bathymetry and the particle tracks are very much in agreement about the location of the watershed. An exception lies in the middle of the leftmost figure. Both the brown and the grey particles do not behave as would have been expected from the bathymetry data. Because the bathymetry data is more definitive about the location of the watershed than the particle data, in this case the bathymetry is more normative than the particle simulation.

If the tidal watersheds are drawn on different scale levels, subbasins of different scales can be identified. The tidal watersheds of the year 2005 are shown in figure 7.

The last step is to combine watersheds into subbasins. In figure 8 the division of the tidal basins of the year 2005 is shown on different scales. This is also done for the years 2011 and 2017. The areas outside the bathymetry data are not part of the subbasins and should therefore be neglected. As the subbasins get smaller, a larger part of the basin cannot be categorized into one of the subbasins. These bifurcations are part of a subbasin of a larger scale but aren't part of a subbasin of a smaller scale. How these parts of the area are handled in the model is clarified in section 5.

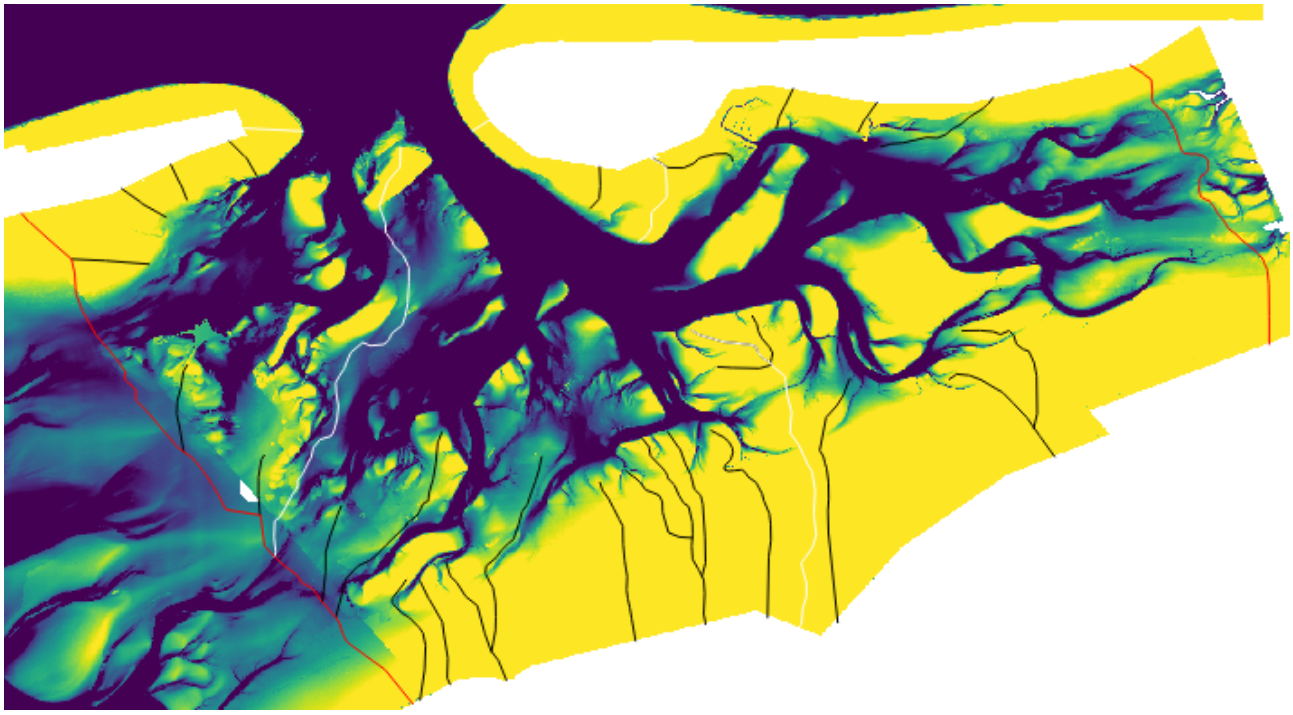

Figure 7: The tidal watersheds in the Ameland Inlet in 2005. The different colors belong to different scale watersheds. The red lines are the main watersheds and the borders of the Ameland Inlet. The white lines are the major watersheds within the Ameland Inlet and the black lines are minor watersheds.

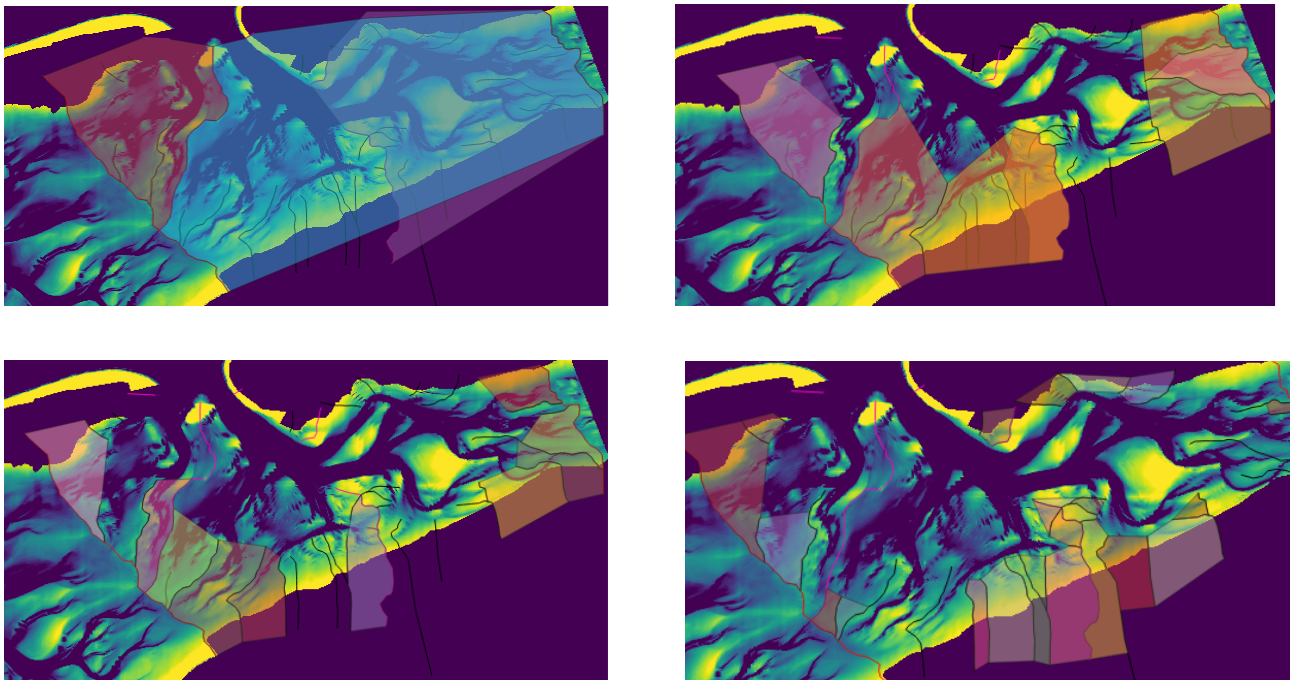

Figure 8: The basins of different scale levels of the Ameland Inlet in 2005

3.4 Hypsometric curve

An easy and fast way to identify the different volumes within the subbasins is by constructing the hypsometric curves. In these curves the percentage of area is plotted against the height that is below that percentage. In figure 9 the hypsometric curves of three basins in the year 2005 are shown.

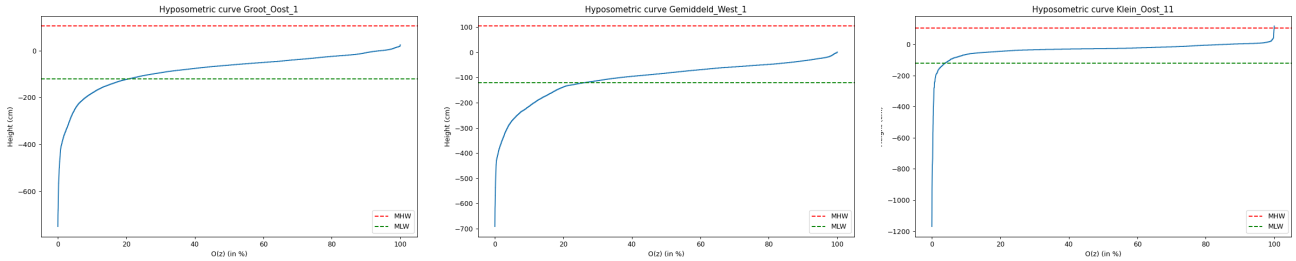

Figure 9: Three examples of hypsometric curves of basins with a different scale level

The Channel Volume (V_c) is in these curves represented by the area below the mean low water (the green dashed line) and above the bathymetry (indicated with the solid blue line). The intertidal flat volume is the area above medium low water and below lowest of the high water (indicated by the dashed red line) and the bathymetry. The Tidal Prism is in these figures illustrated by the area below the high water and above the low water and bathymetry. The different areas in the hypsometric curve are shown in figure 10.

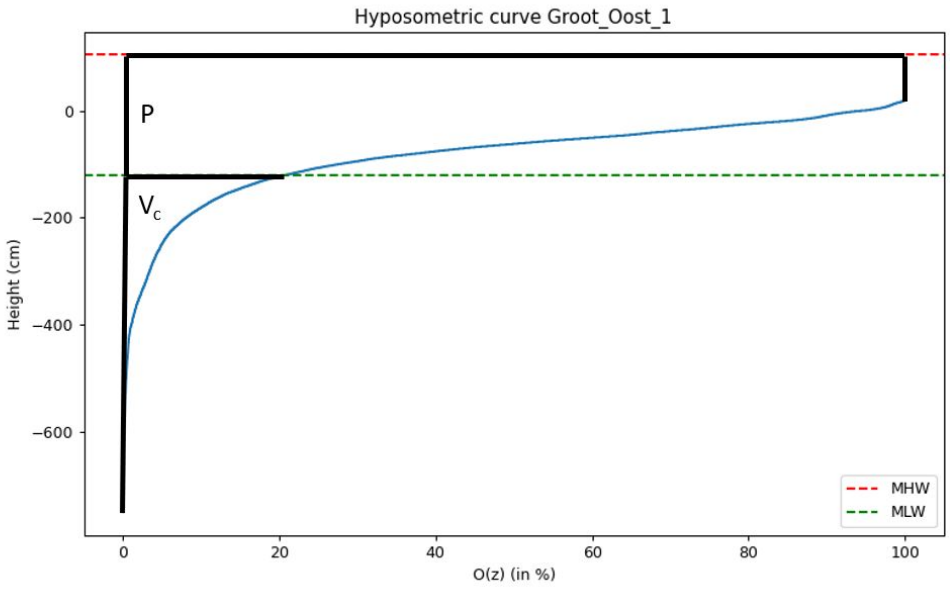

Figure 10: The physical meaning of different areas within a hypsometric curve

From figure 9 some interesting differences in the volumes described in figure 10 can be seen. The channel volume in the third hypsometric curve in figure 9 has a really small channel volume, compared to the other two. A lot more volume is present in the tidal flats over here. These tidal subbasins are on the smallest scale of the fractal system described in subsection 2.5, in this range other (small scale) processes start to play a role in the morphologics of the system.

It is important to find the applicability boundaries in the process of finding a morphological equilibrium relation for between the tidal prism and the channel volume.

3.5 Preliminary results

If the Tidal Prism and Channel Volume of each of the basins of the 2005 situation is obtained using the hypsometric curves, a clear correlation can be observed. This can be seen in figure 11. The figure shows that the deviation of the scatter gets bigger, as the basins get smaller. Basins with a size corresponding to the points in this location in the graph have a channel volume that is relatively small compared to the tidal prism. There are three theories that could explain this behaviour. The first has to do with the grid size of the bathymetry. As the basins get smaller, the channels get smaller. At some point the resolution of the bathymetry plays a part. It could be the case that the flow still uses the small channels in the system, but the channels are too small to be seen in the bathymetry. The second explanation is a physical explanation. It could be that the deviation is caused by the fact that at smaller scales a larger fragment of the flow is over the flats. In this case the channels accommodate a smaller part of the tidal prism and can therefore be smaller with respect to the tidal prism. This could be subject of further research but falls outside of the scope of this study. A third explanation is in line with the subsection 3.6. The dynamic nature of these small subbasins can be to blame for the scatter. As small subbasins move, die out or originate continuously, the scatter could be due to subbasins in one of these conditions. Finally, there are a lot of other physical components that play a role at these scales. Wind driven transport, waves, density driven flows or even large-scale turbulence could play a role in the different nature of smaller basins.

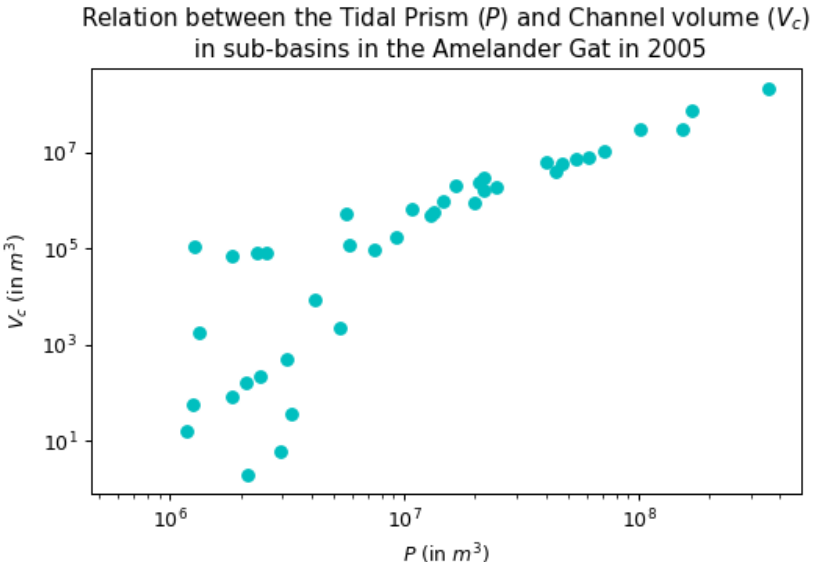

Figure 11: A scatter plot of the channel volume and tidal prism in the Amelander Inlet in the year 2005

The same scatter that is visible in the plot of 2005 in figure 11 is present in the plots of 2011 and 2017 in figure 12. What ever the reason for the scatter might be, it rises some questions about the applicability of the morphological equilibrium. To investigate this, a small research into the applicability of the morphological equilibrium relation found from the data in the plots in figures 11 and 12 is conducted in subsection 3.6.

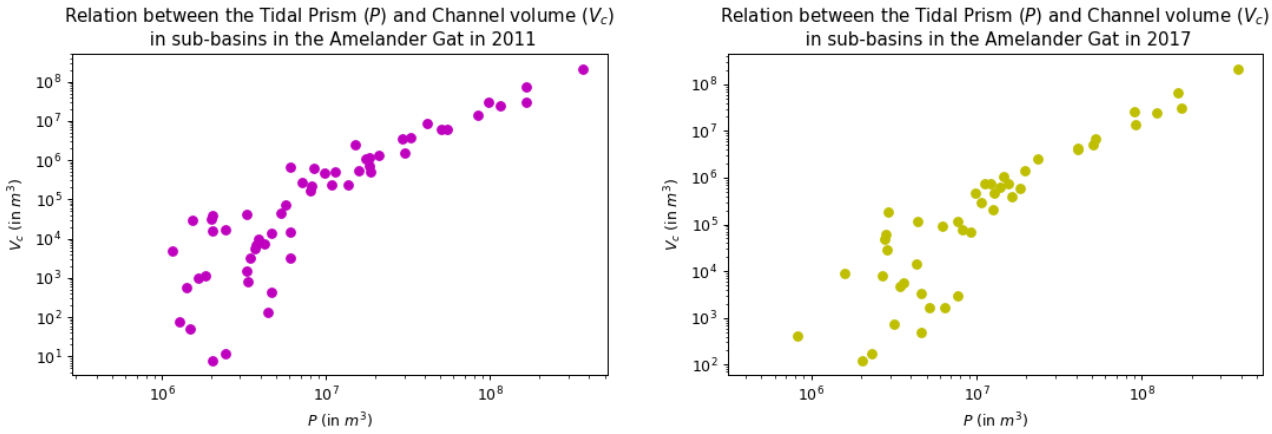

Figure 12: Scatterplots of the channel volume and tidal prism for the years 2011 and 2017

Using the data from all the three years, an equilibrium relation can be obtained.

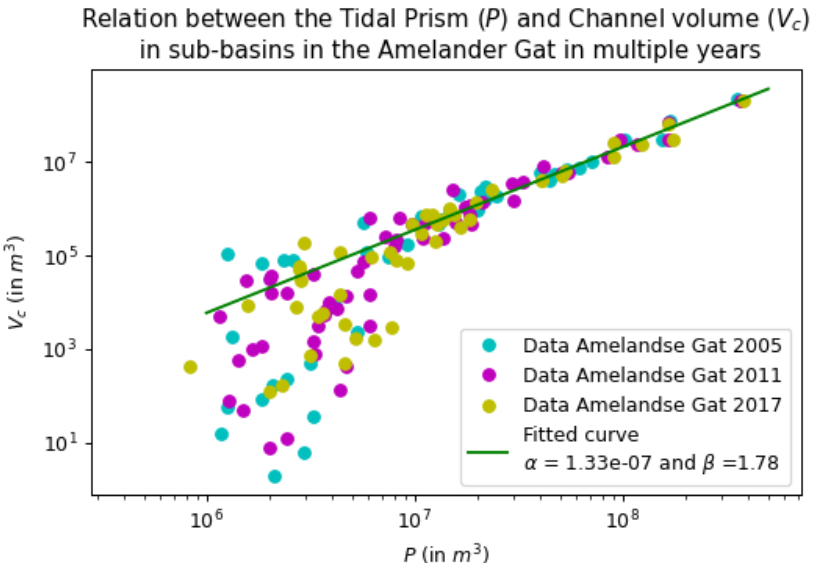

Figure 13: The equilibrium parameters for the relation between the tidal prism and channel volume in subbasins in the Ameland Inlet. All the datapoints in the plot are used for the fitted curve

The equilibrium relation between the tidal prism (P) and the channel volume (V_c) for subbasins in the Ameland Inlet is the following:

$$V_C = 1.33 \cdot 10^{-7} \cdot P^{1.78} \tag{12}$$

3.6 Applicability

As described above, at different scale levels, different processes play a part. Furthermore, an important limitation of the Asmita modelling is that the model uses predefined elements. These predefined elements have a set area and nodal structure. Because of this limitation, the movement of elements and change in its area cannot be represented. This is a problem, especially for the smaller basins. The larger a basins size, the smaller it's relative change in position and

area. The smaller basins are prone to larger (relative) changes. Some further research into the applicability of these relations and the Asmita modelling approach was conducted. Firstly, the constant watershed analysis and secondly the overlap analysis. In this subsection, both are described.

Constant watersheds

The equilibrium relationship for tidal subbasins is determined using a set area during a snapshot of the situation of the tidal subbasin. In reality this area is constantly shifting through the basin and changing in size and shape. In order to examine the robustness of the equilibrium relationship for tidal subbasins, the constant watersheds analysis is conducted.

By keeping the watersheds of the year 2017 of the calibration part of the data-analysis constant and varying the underlying bathymetry, the deterioration of the fit of the newfound morphological equilibrium relation over the years can be investigated. By applying the watersheds of the year 2017 to the bathymetry of the years 1989, 1993, 1999, 2005, 2011 and 2017 and calculating the fit for the different years one can get insight into the deterioration of the fit.

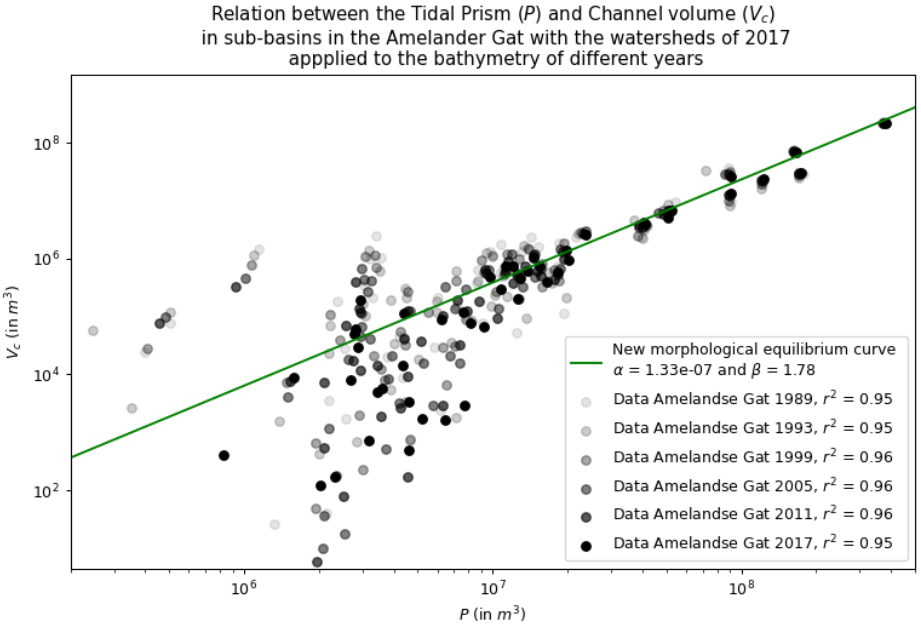

Figure 14: The deterioration of the fit if watersheds of 2017 are applied to different years to the equilibrium relation found in figure 13.

The fit in figure 14 is very good, also if it is applied to the watershed of one year and the bathymetry of the other. The fit doesn't really deteriorate over time.

The optimal size is even a bit more explicitly visible from the plot. The relative deviation over the years of the location of the datapoints for the different basins gets larger as the tidal prism gets smaller. For basins with a tidal prism smaller than $2 \cdot 10^7\ m^3$ the relative deviation becomes significantly bigger.

Overlap analysis

Because of the nodal setup of Asmita, with a predetermined number of elements and prescribed element areas, the model cannot describe the dynamic nature of (especially the smaller) tidal subbasins. To examine the continuity of the positions of different subbasins, the overlap analysis is conducted.

In the overlap analysis the percentual overlap of a basin in between the years 2005, 2011 and 2017 is plotted against the area of the subbasin. A subbasin consists of both a channel and a flat. In the plot a distinction is made in between the percentual overlap after 6 years (2005 and 2011 or 2011 and 2017) and the percentual overlap after 12 years (2005 and 2017).

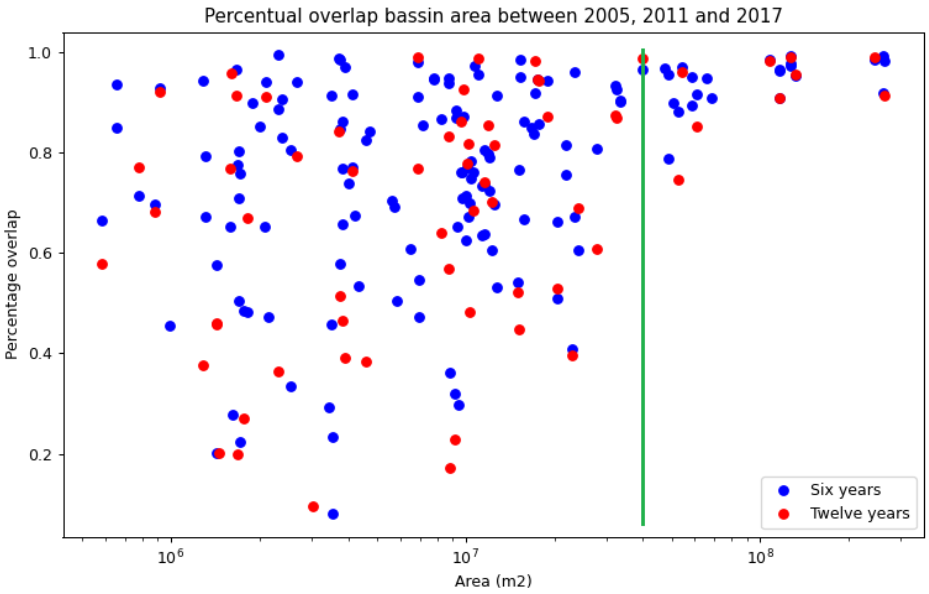

Figure 15: The percentual overlap of basins over the years plotted against its area

It is clearly visible that the overlap is quite substantial for basins with an area of $4 \cdot 10^7$ m^2 (or 40 km^2, the area right of the green line) and larger. The majority of subbasins of 40 km^2 and larger have an overlap of more than 75 %. As the subbasins get smaller than this size, the overlap starts to plummet. This means that larger basins stay more or less in the same spot, while smaller subbasins tend to move a lot more. Because the ASMITA software uses defined subbasins, it is not able to work with subbasins that move too much. The area of a basin and the interchange with other basins is predefined. If the channels of a subbasin move too much, start different links or basins disappear altogether, ASMITA will not be able to forecast the right behaviour. Therefore, the equilibrium relations must be found for and applied to the bigger subbasins.

Conclusion

Both applicability studies have shown that the equilibrium that is the subject of this thesis can only be applied to major tidal subbasins. The criterion provided by both studies differs a bit. From the constant watershed analysis, a minimum tidal prism for the tidal subbasin of $2 \cdot 10^7$ m^3 is found. The overlap analysis dictates a minimum area for a tidal subbasin of 40

km^2. The second criterion is normative, because it limits the applicability more than the other criterion. Due to this criterion, only the largest subbasins within a basin can be used to derive a morphological equilibrium or model a basin.

4 Results equilibrium study

In this section the final results of the equilibrium study described in 3 are described. The criterion of a minimal area of 40 km^2 described in subsection 3.6 is applied to filter the smaller dynamic subbasins and only keep the larger subbasins that are more consistent in their location and area. In the end an equilibrium relation which has a clear applicability limit is derived.

4.1 Conclusion

In all three graphs in figures 11 and 12, the data shows a distinct relation between the channel volume and the tidal prism of a basin. The strong relation for bigger subbasins is very useful in determining an equilibrium relation between the channel volume and the tidal prism. As described in subsection 2.2 we expect the equilibrium formula in the following form:

$$V_C = \alpha_c \cdot P^{\beta_c} \tag{13}$$

Using the criterion from subsection 3.6, a lot of the datapoints in figures 11 and 12 can be filtered. Using criterion in the morphological equilibrium plot for the morphological equilibrium between tidal prism and channel volume, the morphological equilibrium for the more dynamically stable tidal subbasins can be found. In figure 16 the datapoints belonging to basins that do not fit the size criterion are shown with a small cross. The datapoints that do fit the size criterion and are used in determining the morphological equilibrium equation are shown in a solid dot.

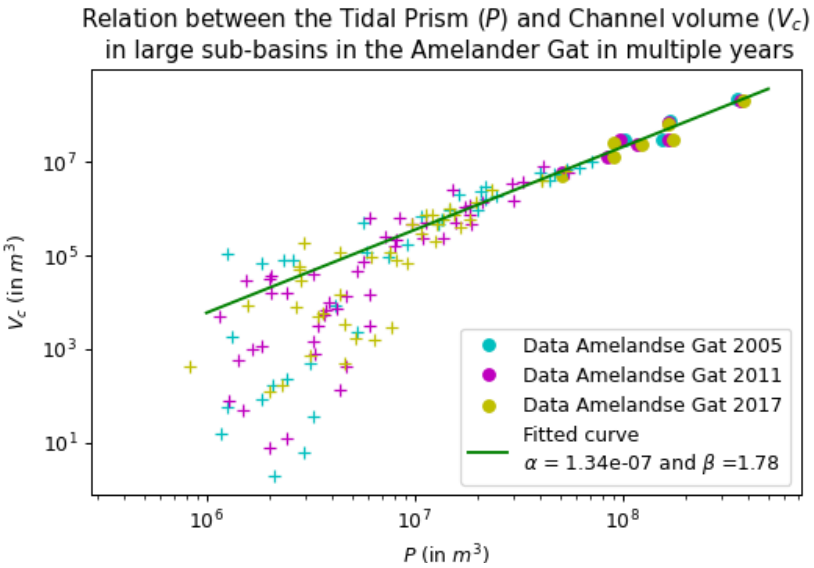

Figure 16: The equilibrium parameters for the relation between the tidal prism and channel volume in subbasins with an area larger than 40 km^2 in the Ameland Inlet. The solid dots pass the criterion and are used for the fitted curve. The crosses are the smaller basins.

The equilibrium relation between the channel volume and tidal prism for dynamically stable subbasins in the Ameland Inlet is the following:

$$V_C = 1.34 \cdot 10^{-7} \cdot P^{1.78} \tag{14}$$

4.2 Application to other basins

To validate the fit found for the larger basins, the basins in the eastern part of the Wadden Sea are evaluated. These basins are a lot smaller than most basins in the Ameland Inlet. They do have the benefit though that the basins should be close to their morphological equilibrium. There are no closures in this part of the Wadden Sea and there is small economic activity, because there are no major waterways and the islands are uninhabited wildlife resorts.

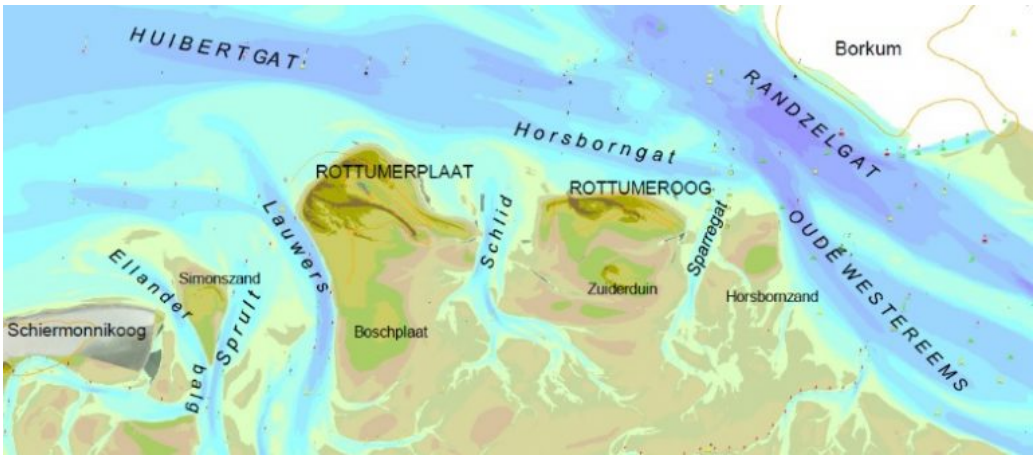

Figure 17: The tidal basins in the Eastern Wadden Sea

The basins in this part of the Wadden Sea are, from west to east, Eilander Balg, Lauwersgat (or Boschgat), Schild, Sparregat, Eemsgat and Uithuizergat. The basins vary in area from 10 to 150 km^2. The tidal watersheds in the area are determined in the same way as for the Ameland Inlet. A particle simulation is done for the entire basin. Using the particle simulation and the bathymetry of the area, the locations of the tidal watersheds are determined.

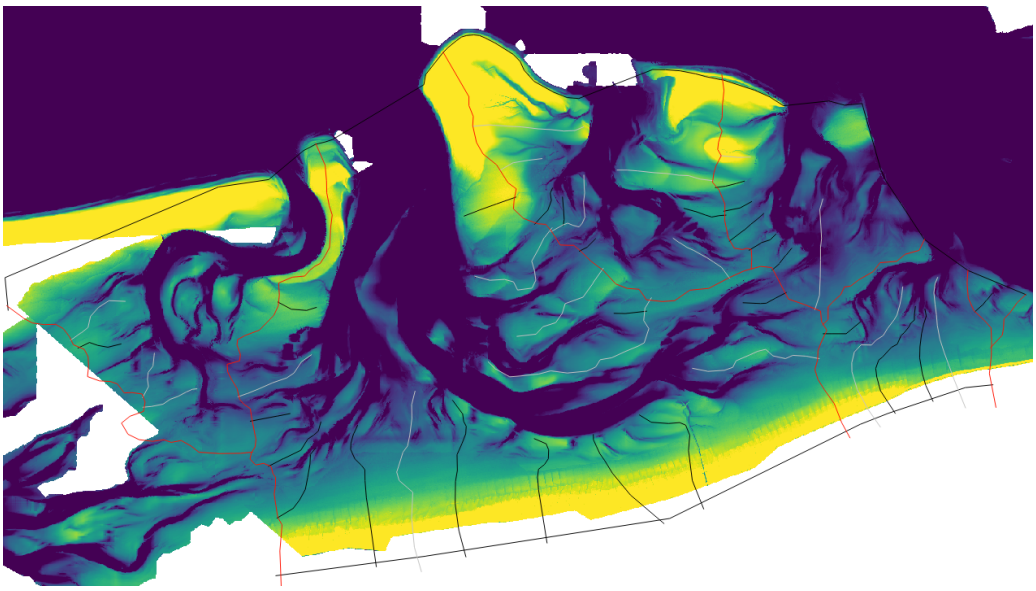

Figure 18: The tidal watersheds in the eastern part of the Wadden Sea. The different colors belong to different scale watersheds. The red lines are the main watersheds and the borders between different basins. The white lines are the major watersheds within the basins and the black lines are minor watersheds.

After constructing the hypsometric curves of the different basins and identifying the different relevant volumes and plotting the results, the fit to the morphological equilibrium relation can be found.

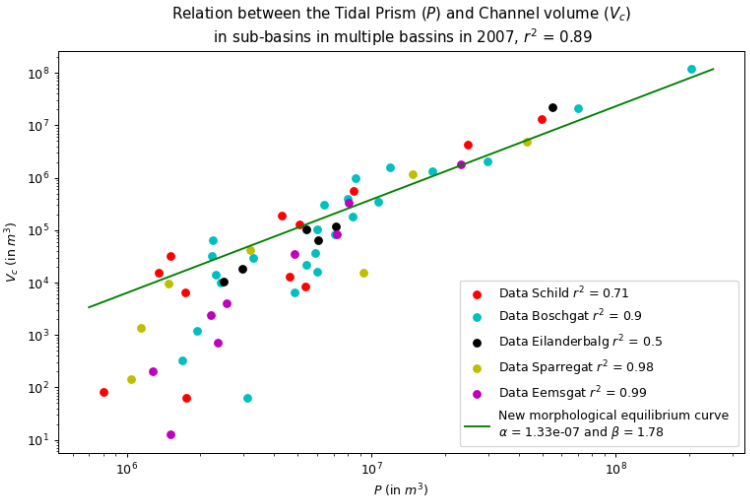

Figure 19: The fit of the small basins in the eastern Wadden Sea to the morphological equilibrium relation found in the Ameland Inlet

Although almost all of the subbasins are smaller than the criterion derived in 3.6, still some interesting things can be derived from this figure. A similar trend as the one in figure 16 is visible in figure 19. For smaller subbasins a lot of scatter is present and the larger subbasins seem to be closer to the newfound equilibrium, although the channel volume is larger with respect to the tidal prism than would be expected from the equation.

The fit is very good for the subbasins of the middle-sized basins. The subbasins of the largest basin have the third best fit, still performing quite well. Two of the basins closest to the mouth of the Ems River have the best fit to the morphological equilibrium relation for tidal subbasins. It is not really possible to derive a conclusion from the differences of the fit of the subbasins within the basins in the eastern part of the Wadden Sea. Larger subbasins have a slightly better fit than smaller subbasins, but the difference is too small to have a hard conclusion.

More research should be conducted before the morphological equilibrium relations are used for subbasins in other basins. While this small exercise does show that larger subbasins in other tidal basins also have some sort of morphological equilibrium and that he equilibrium of the 'Sparregat', 'Eemsgat' and 'Boschgat' is probably very similar to the one found for the Ameland Inlet. Its exact form could be different for different basins due to circumstantial factors.

If looked at figure 19 the scatter is marginal for subbasins with a tidal prism of larger than $1.0 \cdot 10^7\ m^3$. This does not defer to much from the value at which the scatter in figure 16 starts. This suggests that the physical processes that take place and cause this scatter are present in all basins smaller than this value and are thus very size dependent. The relative size of the subbasin with respect to the entire basin does not play a big role, as the basins in figure 19 are way smaller than the Ameland Inlet. It also suggests that the applicability criterion of the basin might be very similar to the one found in subsection 3.6, but it is only possible to make a definitive conclusion about this if the same process is executed as was in this subsection.

5 Method multiple element Asmita modelling

In order to be able to investigate the partial differences in morphological behaviour between different parts of the basin, a modelling exercise is done. The results of this modelling exercise are described in section 6. In this section the most important differences in parameter setting compared to the original parameter setting (Wang et al., 2018) for the 3-element model are described.

This modelling exercise is not done in Asmita software, but in a test code version of the Asmita model in Matlab. This is because the Asmita software is not yet able to work with the tidal prism of a subbasin. In future work this should be added as an option to the Asmita software. In this test code the found equilibrium relation in section 4 is applied to find the volumes of the channel elements in subbasins. The test code of the 3-element model is in appendix C. The code of the 6 and 10 element models are in appendices D and E respectively.

5.1 6 element model

The six-element model is the closest neighbour to the original three element model. In order to come to this model, the original three element model was used as basis. The ebb tidal delta and its properties were not changed. The original flat element was split up into two elements, a western and eastern flat element. The original channel element was split up into three elements. An east element, a west element, and a bifurcation element. The subdivision is shown in figure 20. In the figure the ebb tidal delta is shown in green, the bifurcation channel in purple, the west channel and flat element in orange and the east channel and flat element in red. A sketch of the borders inbetween the channels and flats is drawn in the figure. The western and eastern elements in this figure are subdivided into a channel and flat part, with the area's that are permanent flooded being part of the channel and the other areas belonging to the flats.

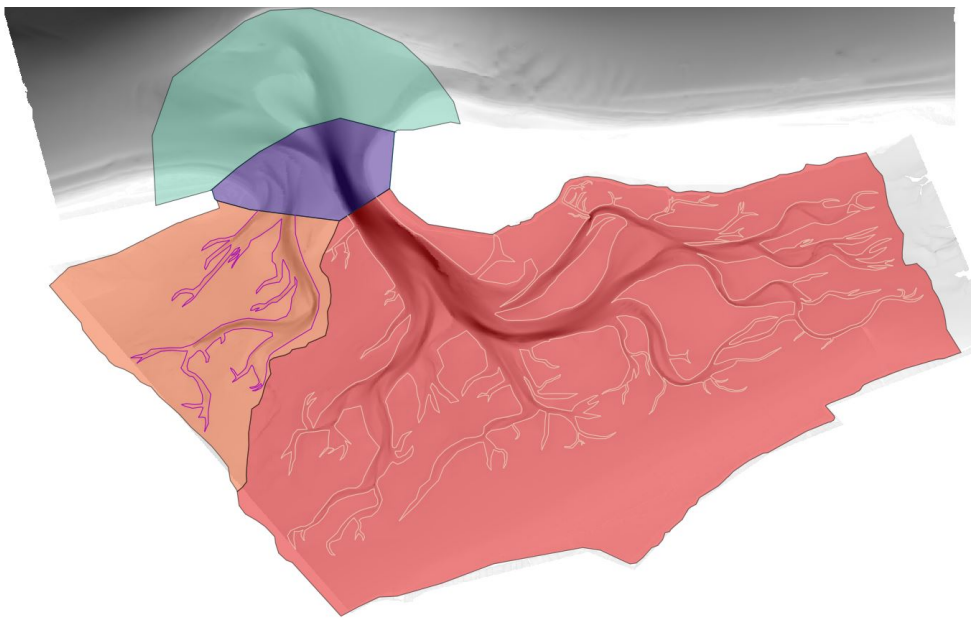

Figure 20: The subdivision of elements in the 6-element model. In this figure, the borders of the channels are sketched, while in the model the area is divided along the depth. Areas where the sea bed is lower than MLW belong to the channels and areas that are higher than MLW belong to the flats.

The settings in this research have been kept consistent with the settings for the Ameland Inlet as described in a study done by Wang Wang et al. (2018) if possible. In cases that this was not the case, the parameter choice is described below. The used parameters for the simulations are given in table 1. The area of the channels and the flats in the 3-element model is $27.6 \cdot 10^7$ this is just a little bit larger than the area of all channel and flat elements in the 6-element model, which has an area of $27.3 \cdot 10^7$. The difference lies entirely in the flats.

	Area m^2	**Volume** m^3	**Vertical exchange** m/s
Ebb tidal delta	$7.5{\cdot}10^7$	$1.3{\cdot}10^8$	$1.0{\cdot}10^{-5}$
Bifurcation channel	$5.0{\cdot}10^6$	$3.4{\cdot}10^7$	$5.0{\cdot}10^{-5}$
West channel	$2.6{\cdot}10^7$	$3.9{\cdot}10^7$	$5.0{\cdot}10^{-5}$
West flat	$3.5{\cdot}10^7$	$1.3{\cdot}10^7$	$1.0{\cdot}10^{-4}$
East channel	$6.7{\cdot}10^7$	$2.3{\cdot}10^8$	$5.0{\cdot}10^{-5}$
East flat	$1.4{\cdot}10^8$	$1.1{\cdot}10^8$	$1.0{\cdot}10^{-4}$

Table 1: Element properties based on the bathymetry of 2017 of the Ameland Inlet of the 6-element model

The areas and volumes from table 1 are subtracted from the bathymetry data of 2017 using the subdivision of the coloured planes visible in figure 20 in QGIS. The subdivision between channels and volumes is done along the depth of the area. The values for the vertical exchange are the same as in the values used for the run with 3 elements.

As both the area of the west channel and west flat combined and the east channel and east flat combined are higher than 40 km^2, it fits the criterion given in subsection 3.6 and the subbasins are not too small to model. In the model, different equilibria are used for different elements:

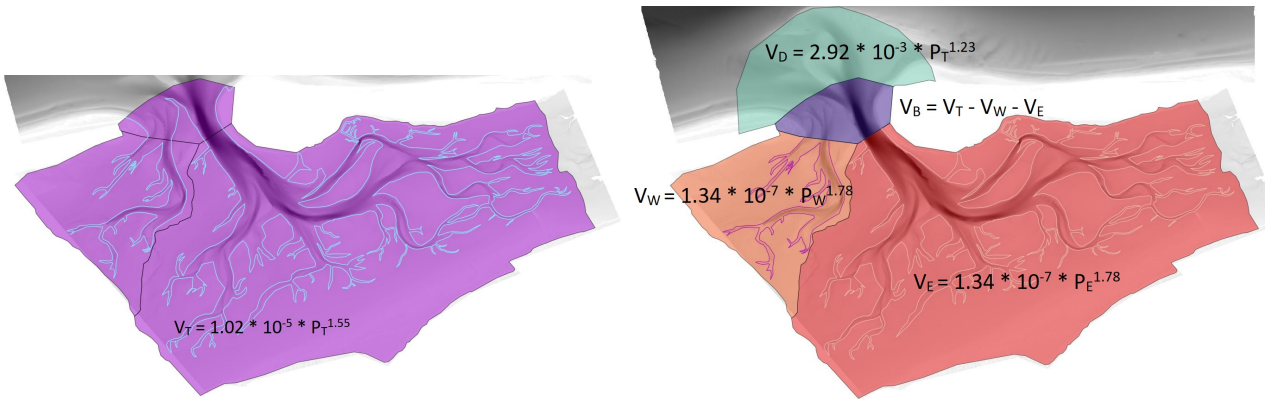

Figure 21: Global and local equilibrium relations in 6 element model of the Ameland Inlet

The equation for the ebb tidal delta doesn't differ from the equation used in the 3-element model:

$$V_D = 2.92 \cdot 10^{-3} \cdot P_D^{1.23} \tag{15}$$

The equations for the western and eastern part of the basin are also quite straightforward. The

equations for the equilibrium of a subbasin found in the data-analysis of this thesis are used for the western and eastern subbasins:

$$V_C = 1.34 \cdot 10^{-7} \cdot P_C^{1.78} \tag{16}$$

In which the used tidal prisms (P_C) are the tidal prisms of the eastern and western subbasin. There is no equilibrium volume for a bifurcation element. To find the equilibrium volume of a bifurcation element, two steps are undertaken. First the equilibrium volume of the channels in the entire basin (V_T) is calculated. This is done using the equilibrium relation for entire basins. The channel volumes of the Eastern and Western elements (V_W and V_E), determined using the new morphological equilibrium relation, are subtracted from this total volume, to find the volume of the remaining part of the basin (V_B, for the bifurcation element).

$$\begin{aligned} V_T &= 1.02 \cdot 10^{-5} \cdot P_T^{1.55} \\ V_B &= V_T - V_W - V_E \end{aligned} \tag{17}$$

The equilibrium volumes of the intertidal flats are determined using equation 4. A last parameter that should be determined, that differs from the values used in the three-element model is the horizontal exchange coefficient $\delta_{i,j}$. The way in which the horizontal exchange is determined is described in a paper about the background to Asmita (Townend et al., 2016). This horizontal exchange is determined in two steps first, the dispersion coefficient (D) is determined in the following way:

$$D = \epsilon \frac{u^2 H}{w} \tag{18}$$

In this equation u is the scale of the tidal flow velocity, H is the hydraulic water depth and w is the rate of of vertical exchange. The coefficient of proportionality of ϵ is a calibration parameter with a value of around 0.1 this us used to guarantee the right level of mixing. The dispersion coefficient is subsequently used in order to determine the horizontal exchange:

$$\delta_{i,j} = \frac{D_{i,j} A_{i,j}}{\Delta x} \tag{19}$$

The horizontal exchange is determined for every link in between two elements. The wet cross-sectional area ($A_{i,j}$) and distance (Δx) between two elements are used in order to find the horizontal exchange parameters. Some of the values in this process are in the same scale as a physical parameter or a calibration coefficient. These values are determined using field observations. This process is described in a paper (Wang et al., 2008). Because of the difficulties of the parameter setting in determining the parameter setting for the horizontal exchange, this thesis uses the values of the paper of Wang et al. (2018) as a basis and determines the differences in the process of determining the horizontal exchange. An assumption is made that the value of the dispersion coefficient does not change if an element is subdivided into multiple elements. This simplifies the process of finding the values of the horizontal exchange to finding the differences in horizontal area and distance between two elements:

$$\delta_{6EM} = \delta_{3EM} \cdot \left(\frac{\Delta x_{3EM}}{\Delta x_{6EM}}\right) \cdot \left(\frac{A_{6EM}}{A_{3EM}}\right) \tag{20}$$

This equation is used to calculate the value for the horizontal exchange for every link in between elements of the six-element model. The values for the cross-sectional area and the distance in between two elements are found in QGIS. The way in which the elements are linked is shown in figure 22. The values for the horizontal exchange in between the elements are also given in the figure. The values for the horizontal exchange are an estimation based on the values of the original 3 element model. A more extensive investigation in appropriate values for this parameter should be done in future research.

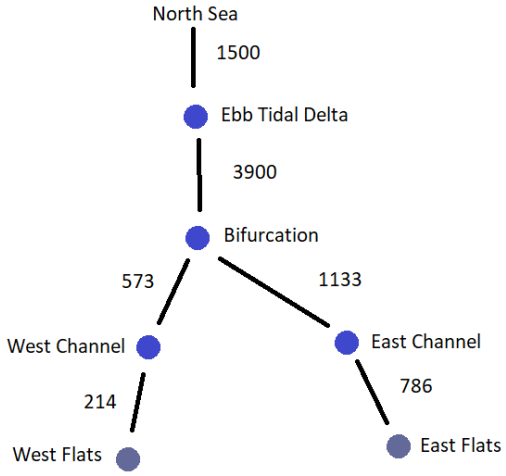

Figure 22: The horizontal exchange in the 6-element model (in m^3/s)

5.2 10 element model

The 10-element model is based on the 6-element model described in this chapter. The eastern element in the 6-element model is split up into three new elements. Another bifurcation, the mid element, and the far eastern element. The subdivision of the elements is shown in figure 23.

The areas of the elements within the basin (the green 'western', orange 'mid', yellow 'bifurcation 2' and purple 'far east' elements) are subdivided into channel and flat elements according to the depth of the area. The channel elements and the tidal flat elements are visible in figure 23, in this figure the channel elements are sketched, while in reality the elements are divided along the depth. The areas where the sea surface is between MHW and MLW belonging to the flats and the areas that are below MLW belonging to the channels. The used parameters of the model are shown in in table 2. The total area of the channel and flat elements in the 3-element model is $27.6 \cdot 10^7 m^3$. If all the channel and flat areas of the 10-element model are added up they have a total of $27.8 \cdot 10^7 m^3$. Both the channels and flats are approximately $0.1 \cdot 10^7 m^3$ larger in the 10-element model than in the original model.

As is the case with the six-element model, if for every subbasin the area of the channel and flats are combined, it adds up to a value excess of 40 km^2. All the subbasins fit the criterion given in subsection 3.6 and the subbasins are not too small to model. The areas for the subbasins in

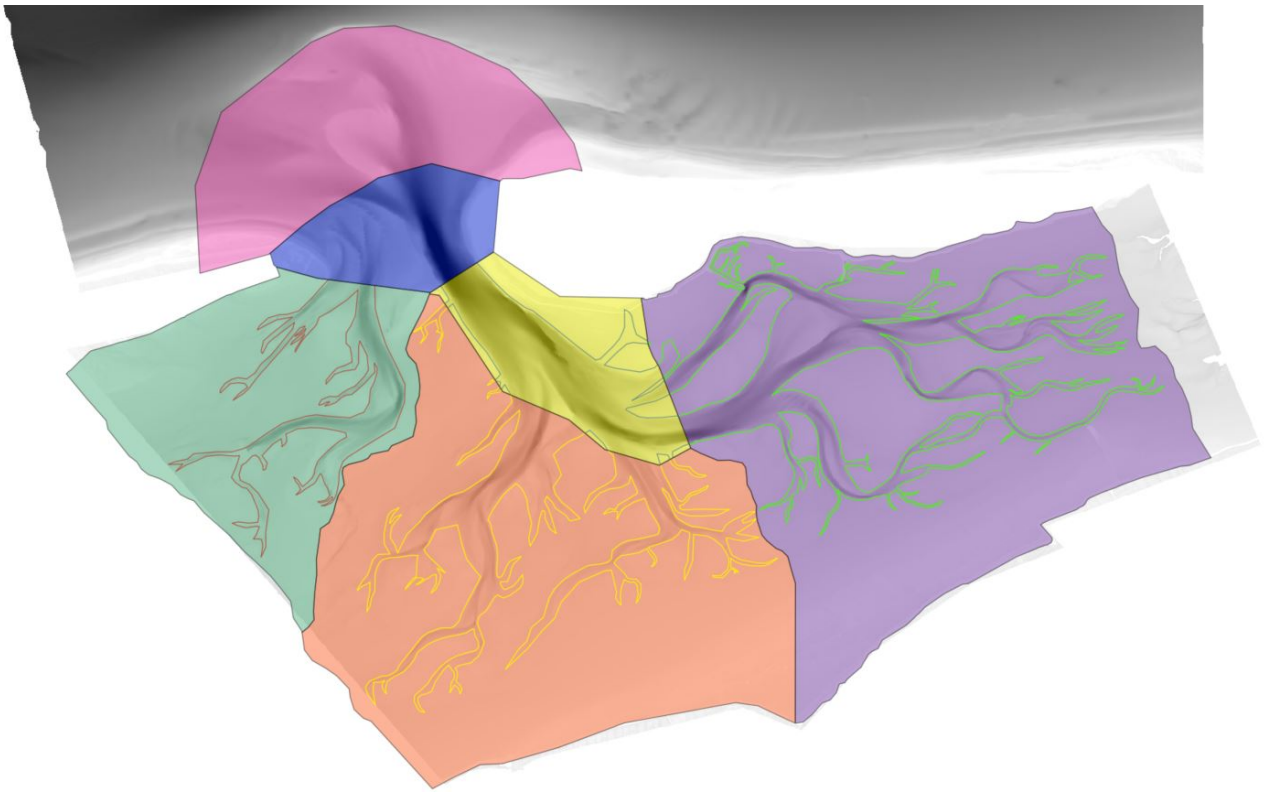

Figure 23: The subdivision of elements in the 10-element model. In this figure, the borders of the channels are sketched, while in the model the area is divided along the depth. Areas where the sea bed is lower than MLW belong to the channels and areas that are higher than MLW belong to the flats.

	Area m^2	**Volume** m^3	**Vertical exchange** m/s
Ebb tidal delta	$7.5 \cdot 10^7$	$1.3 \cdot 10^8$	$1.0 \cdot 10^{-5}$
Bifurcation channel	$5.0 \cdot 10^6$	$3.4 \cdot 10^7$	$5.0 \cdot 10^{-5}$
West channel	$2.6 \cdot 10^7$	$3.9 \cdot 10^7$	$5.0 \cdot 10^{-5}$
West flat	$3.5 \cdot 10^7$	$1.3 \cdot 10^7$	$1.0 \cdot 10^{-4}$
Bifurcation II channel	$1.1 \cdot 10^7$	$1.2 \cdot 10^8$	$5.0 \cdot 10^{-5}$
Bifurcation II flat	$2.8 \cdot 10^6$	$2.3 \cdot 10^6$	$1.0 \cdot 10^{-4}$
Mid channel	$2.8 \cdot 10^7$	$3.8 \cdot 10^7$	$5.0 \cdot 10^{-5}$
Mid flat	$6.5 \cdot 10^7$	$4.5 \cdot 10^7$	$1.0 \cdot 10^{-4}$
Far East channel	$2.9 \cdot 10^7$	$7.6 \cdot 10^8$	$5.0 \cdot 10^{-5}$
Far East flat	$7.6 \cdot 10^7$	$6.1 \cdot 10^7$	$1.0 \cdot 10^{-4}$

Table 2: Element properties based on the bathymetry of the Ameland Inlet of 2017 of the 10-element model

this model are in the same order of magnitude as the criterion value. Theoretically the mid and far east subbasins could still be divided in two areas and fit the criterion, but it is impossible to identify in figure a watershed that creates good tidal subbasins in these areas 7. This model is the most detailed model which could be made in the Ameland Inlet using the equilibrium volume approach.

The equilibria in the 10-element model work quite alike the equilibria in the 6-element model displayed in figure 21. The same method is used, but it goes one step further. The western and first bifurcation equilibria still hold. The eastern equilibrium in this figure is split in a similar way as the total equilibrium was in the 6-element model. This is shown in figure 24 and equation 21.

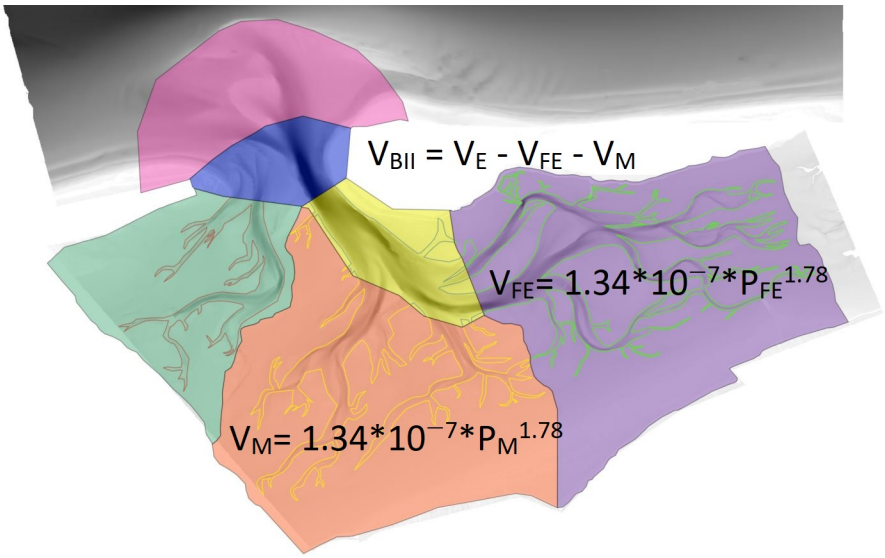

Figure 24: The locally used equilibria in the eastern part of the Ameland Inlet

$$\begin{aligned} V_E &= 1.34 \cdot 10^{-7} \cdot P_E^{1.78} \\ V_{FE} &= 1.34 \cdot 10^{-7} \cdot P_{FE}^{1.78} \\ V_M &= 1.34 \cdot 10^{-7} \cdot P_M^{1.78} \\ V_{BII} &= V_E - V_{FE} - V_M \end{aligned} \tag{21}$$

As is the case with the six-element model, in the ten elements model the equilibrium volume of the tidal flats is divided proportionally to the areas of all flat elements. The horizontal exchange ($\delta_{i,j}$) is extracted in a similar way as was done with the 6-element model in subsection 5.1. The resulting values are visualised in figure 25.

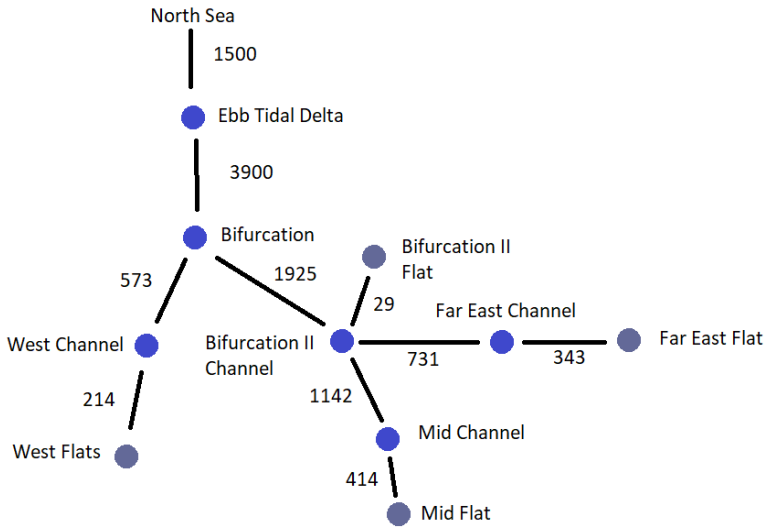

Figure 25: The horizontal exchange in the 10-element model (in m^3/s)

6 Results multiple element Asmita modelling

In this section the results generated by the multiple element Asmita modelling, as described in section 5 are being discussed. Both the 6 and 10 element models will be assessed. For both models 3 simulations are discussed. Firstly, a simulation without sea level rise, the static equilibrium. Secondly, a simulation with a sea level rise of 2 mm/year, which is the closest case to present-day sea-level rise. And finally, a simulation with a sea level rise of 8 mm/year, which will represent a probable sea level rise in the year 2050. The starting time (T_0) in all of the simulations in this section is the year 2017. The volumes and areas of different subbasins are based on this year. It should be noted that all delta and flat volumes in this section are sediment volumes while all channel volumes are water volumes.

6.1 6 element model

The results given by the modelling described in subsection 5.1, using six elements, are presented in this subsection. The situations without sea level rise and with 2 mm/year and 8 mm/year sea level rise are examined, as stated above. The results for 4 and 6 mm/year sea level rise can be found in Appendix A.

No sea level rise

In order to check the results of the modelling with a six-element model and without sea level rise, the outcome of the new model is compared to the outcome of the original three element model. In the comparison, the equivalent elements of the six-element model are plotted with the original element of the three-element model. The result of this comparison is used to check the new model. The comparison, in figure 26, shows that the six-element model is capable of generating equivalent results to the original model, although there are some differences in the response. The resulting equilibrium of both models is exactly the same, because the same equilibrium is prescribed and the horizontal exchange does not influence the morphological equilibrium. In the case of a dynamic equilibrium the horizontal exchange could make a difference to the morphological equilibrium. The timescales of both models are also very close to each other. The biggest difference between both models is in the timescale of the Delta element. The 6-element model converges to the equilibrium value in approximately 160 years as opposed to the original model, which reaches its equilibrium in approximately 200 years.

The goal of the six-element model is to investigate the morphological behaviour and equilibrium on a smaller scale. By plotting the volume of the six individual elements over time, this can be visualised.

Figure 27 and table 3 show that the different areas in the basin act differently in this simulation. The eastern flats are way closer to their equilibrium than the western ones. The increase in volume of the flats in the basin is entirely due to the western part of the flats. The eastern flats decrease in size a bit. In the channels the behaviour of the western and eastern part is more similar. Both elements decrease in size about the same amount. Relative speaking, the decrease in the western part more substantial, because this element is significantly smaller than the eastern part. The bifurcation, on the other hand, increases in size a little bit. The Delta increases in volume, as it does in the original 3 element model. The increase in volume of the delta is negligible relative to the starting and final volume of the element.

The simulation without sea level rise delivers very valuable information. Without sea level rise,

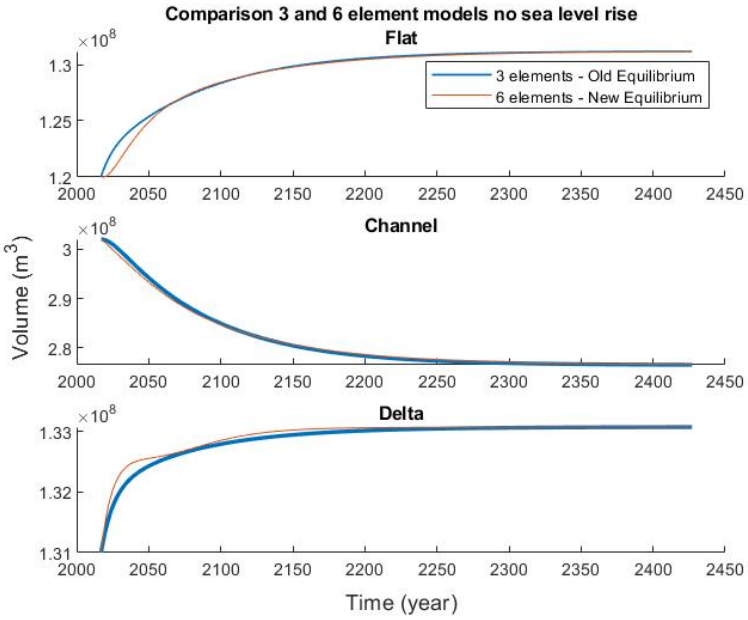

Figure 26: A comparison between the original 3 element and new 6 element model

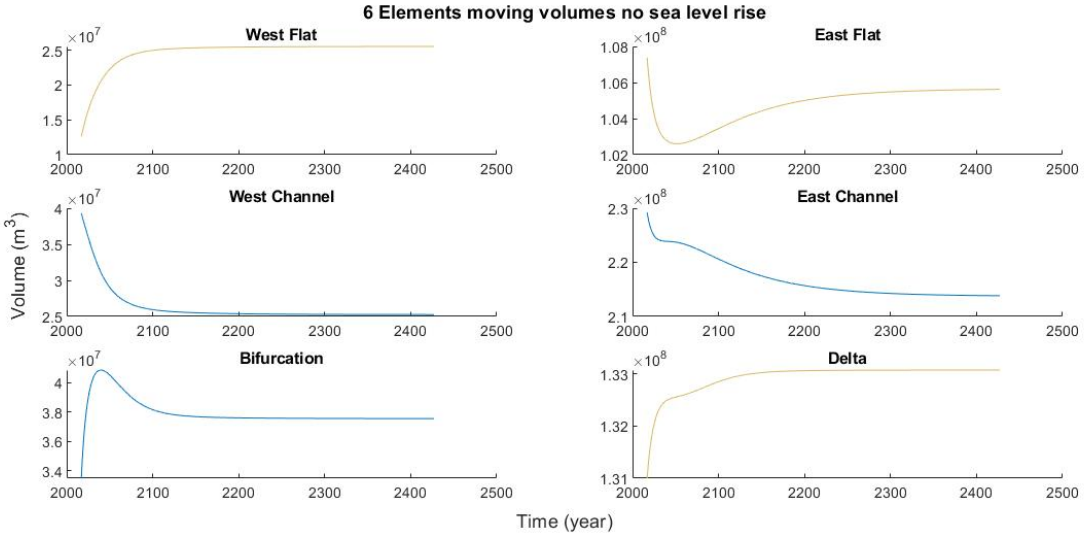

Figure 27: The change in volume of all elements in the 6-element model. Water volumes are blue and sand volumes are yellow.

the static equilibrium will establish in the end. This simulation shows how far each element is from its static equilibrium.

	Flats		**Channels**			**Delta**
	West	*East*	*West*	*East*	*Bifurcation*	
Begin	$1.3 \cdot 10^7$	$1.1 \cdot 10^8$	$3.9 \cdot 10^7$	$2.3 \cdot 10^8$	$3.4 \cdot 10^7$	$1.3 \cdot 10^8$
End	$2.6 \cdot 10^7$	$1.1 \cdot 10^8$	$2.5 \cdot 10^7$	$2.1 \cdot 10^8$	$3.8 \cdot 10^7$	$1.3 \cdot 10^8$
Difference	$1.3 \cdot 10^7$	$-1.7 \cdot 10^6$	$-1.4 \cdot 10^7$	$-1.5 \cdot 10^7$	$4.1 \cdot 10^6$	$2.1 \cdot 10^6$

Table 3: The starting, final and difference in volume (in m^3) of all the elements in the 6-element simulation without sea level rise

In the western part of the basin, both the flats and the channels encounter sedimentation and thus a sediment import. In the eastern part of the basin, the flats have a tiny bit of erosion, but the dominant factor is the sedimentation in the eastern channel. The bifurcation has a little bit of erosion and the delta a little bit of sedimentation. In total there is a sediment import of $3.8 \cdot 10^7\ m^3$.

2 mm sea level rise per year

The model can also be used in order to study the behaviour of the basin under sea level rise. As the sea level rises, a dynamic equilibrium commences. The reaction of the basin to sea level rise, is to import sediment, to keep up with sea level rise. It will react constantly to the sea level rise. The dynamic equilibrium will depend on the rate of sea level rise and the the transport into the basin. If the transport is not sufficient, the increase in bed level will not be able to keep up with the increase in sea level and the basin will drown. In this section the model will be studied under the influence of sea level rise. For this study, the 2 mm/year and 8 mm/year scenarios are used, in order to meet the current sea level rise and a value which is well within the possibilities for the sea level rise in 2050. In future research even more extreme scenario's may be investigated.

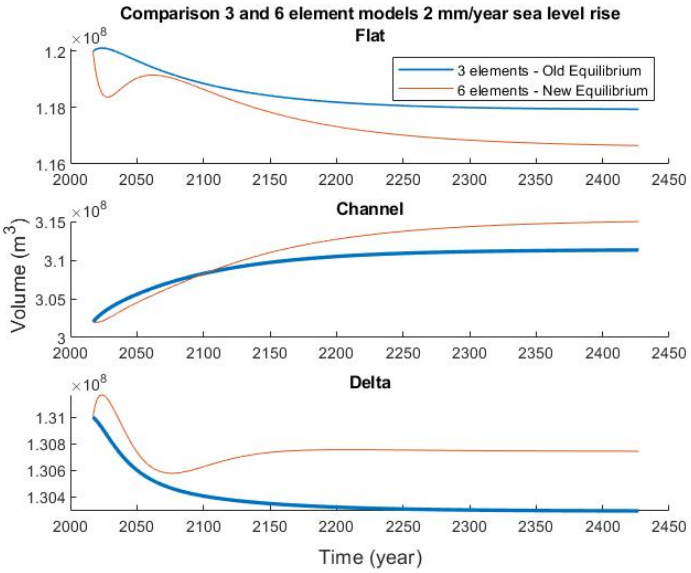

Figure 28: A comparison between the original 3 element and new 6 element model under 2 mm/year sea level rise. Water volumes are blue and sand volumes are yellow.

First the model with 2 mm sea level rise is investigated. This sea level rise is quite representative for the present-day situation. The comparison of equivalent elements is made, like the case without sea level rise beforehand. The result is shown in figure 28.

The result of the original 3 element model is not reproduced well under 2 mm/y sea level rise. As the dynamic equilibrium is way more sensible for the values of the horizontal exchange, an explanation probably lays within these values. The general direction of the equilibria is captured quite well, but there is some difference in the magnitude of the different volumes. The difference in the graphs looks substantial, but if the percentual differential differences are analysed, the actual differences are not that large. Improvement could be made in the representation of the behaviour of the basin under 2 mm/y sea level rise by the six-element model.

	Flats	**Channels**	**Delta**
Final moving value 3EM	$1.2 \cdot 10^8$	$3.1 \cdot 10^8$	$1.3 \cdot 10^8$
Final moving value 6EM	$1.2 \cdot 10^8$	$3.2 \cdot 10^8$	$1.3 \cdot 10^8$
Difference	$-1.3 \cdot 10^6$	$3.7 \cdot 10^6$	$4.5 \cdot 10^5$
Percentual difference	-1.1%	1.2%	0.35%

Table 4: Comparison of the equilibrium volumes between the original model and the 6-element model for 2 mm/year sea level rise. All the values except from the percentages are in m^3.

Opposed to the case without sea level rise, the channels in the system get larger instead of smaller. The flats decrease in size, instead of increase. The ebb tidal delta decreases in size, while it would grow without sea level rise, though in both cases the changes are ever so slightly.

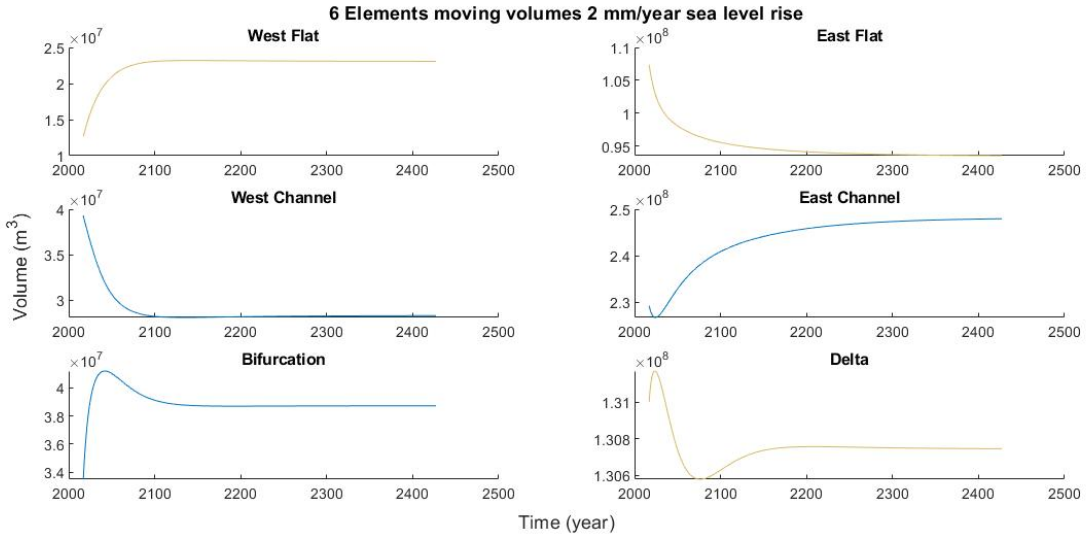

Figure 29: The change in volume of all elements in the 6-element model under 2 mm/year sea level rise

The decrease in volume of the flats, visible in figure 29 and table 5 is solely because of the decrease in volume of the flats in the eastern basin. The flats in the western basin increase in volume. The same holds for the channels. The increase of volume of the channels in the entire basin is almost solely due to the channels in the eastern part of the basin. There is a smaller

contribution of the bifurcation and the western part of the channels have a tendency contrary to the contribution of the eastern part.

	Flats		**Channels**			**Delta**
	West	*East*	*West*	*East*	*Bifurcation*	
Begin	$1.3 \cdot 10^7$	$1.1 \cdot 10^8$	$3.9 \cdot 10^7$	$2.3 \cdot 10^8$	$3.4 \cdot 10^7$	$1.3 \cdot 10^8$
End	$2.3 \cdot 10^7$	$9.4 \cdot 10^7$	$2.8 \cdot 10^7$	$2.5 \cdot 10^8$	$3.9 \cdot 10^7$	$1.3 \cdot 10^8$
Difference	$1.0 \cdot 10^7$	$-1.4 \cdot 10^7$	$-1.1 \cdot 10^7$	$1.9 \cdot 10^7$	$5.2 \cdot 10^6$	$-2.6 \cdot 10^5$

Table 5: The starting, final and difference in volume (in m^3) of all the elements in the 6-element simulation with 2 mm/year sea level rise

The channels in the western part of the basin decrease and the flats increase in size. The influence of sea level rise is easily encountered by a sediment import in this part of the basin. In the eastern part, the channels increase and the flats decrease in size. This is allready more typical for a basin that is under the influence of sea level rise. The bifurcation getting larger and the Delta getting smaller instead of larger are both a clear influence of sea level rise. The basins loses a total of $1.7 \cdot 10^7$ m^3 of sediment during the simulation. An import of $2.5 \cdot 10^8$ m^3 sediment almost balances the extra volume of water of $2.7 \cdot 10^8$ m^3 due to sea level rise.

8 mm sea level rise per year

The comparison between the 3 and 6 element models for the case with 8 mm sea level rise per year shows that the order of magnitude is represented quite well by the 6-element model. The results of the first 100-160 years of the flats and channels are very similar to the 3-element model. For the delta this is only 70 years. The timescale of the eb tidal delta differs more than the other parameters. In approximately 200 years the morphological equilibrium is reached for the delta, while the other timescales of both the 3 and 6 element models are not even within the timescale of this graph.

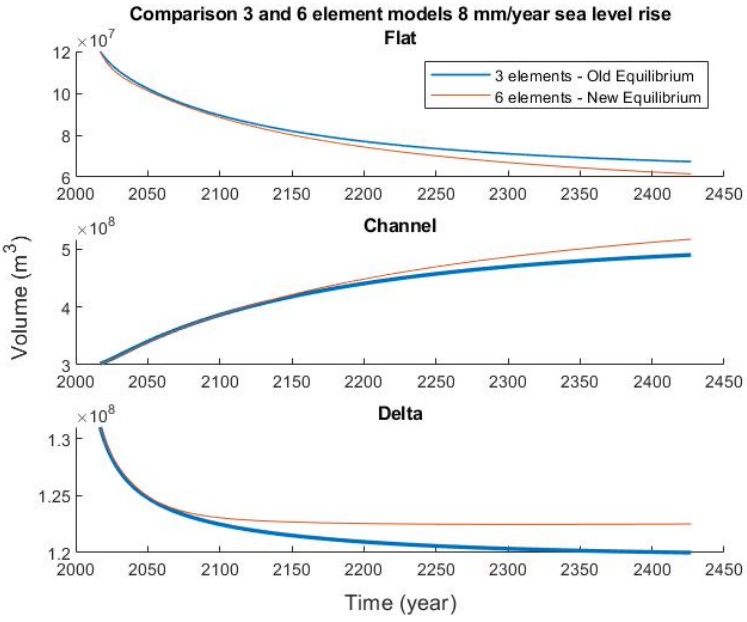

Figure 30: A comparison between the original 3 element and new 6 element model under 8 mm/year sea level rise

The relative error becomes larger as the sea level rise becomes bigger. The tendencies already visible in the models with less sea level rise are also present in this model, with the flats decreasing in volume, the channels increasing in volume and the ebb tidal delta decreasing in volume.

	Flats	**Channels**	**Delta**
Final moving value 3EM	$6.7 \cdot 10^7$	$4.9 \cdot 10^8$	$1.2 \cdot 10^8$
Final moving value 6EM	$6.2 \cdot 10^7$	$5.2 \cdot 10^8$	$1.2 \cdot 10^8$
Difference	$-5.8 \cdot 10^6$	$2.7 \cdot 10^7$	$2.5 \cdot 10^6$
Percentual difference	-8.7%	5.5%	2.1%

Table 6: Comparison of the equilibrium volumes between the original model and the 6-element model for 8 mm/year sea level rise. All the values except from the percentages are in m^3.

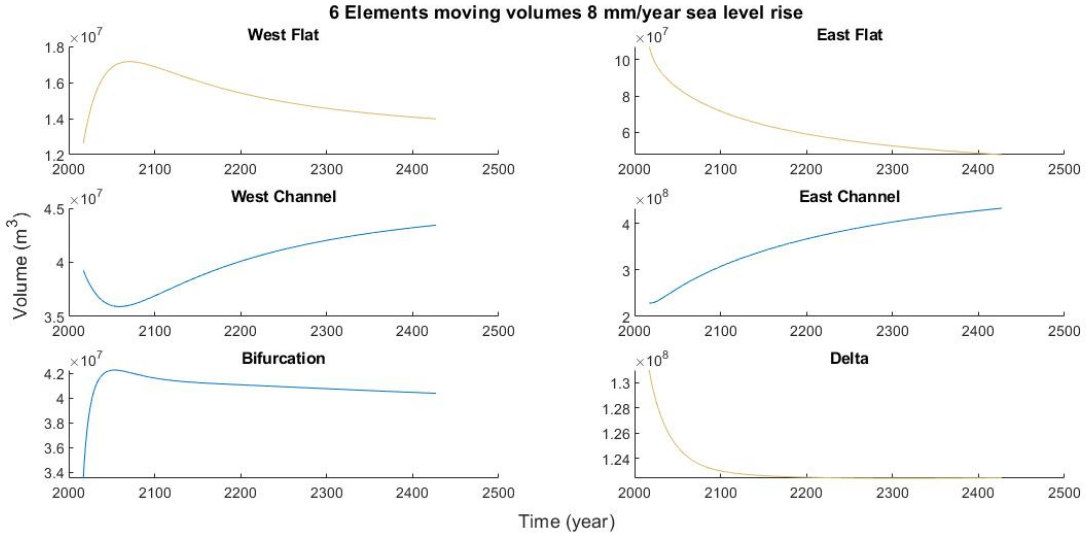

Figure 31: The change in volume of all elements in the 6-element model under 8 mm/year sea level rise. Water volumes are blue and sand volumes are yellow.

The changes in volume of the flats and channels in the basin are mostly due to the eastern parts. The flats decrease and the channels increase in size quite substantially in this part of the basin. The final volume of the eastern flat is less than half of its starting value and the volume of the eastern channels almost doubles in the 400 simulated years. The growth of the west and bifurcation channels is quite substantial, while there is a small growth in the western flats.

	Flats		**Channels**			**Delta**
	West	*East*	*West*	*East*	*Bifurcation*	
Begin	$1.3 \cdot 10^7$	$1.1 \cdot 10^8$	$3.9 \cdot 10^7$	$2.3 \cdot 10^8$	$3.4 \cdot 10^7$	$1.3 \cdot 10^8$
End	$1.4 \cdot 10^7$	$4.8 \cdot 10^7$	$4.3 \cdot 10^7$	$4.3 \cdot 10^8$	$4.0 \cdot 10^7$	$1.2 \cdot 10^8$
Difference	$1.4 \cdot 10^6$	$-6.0 \cdot 10^7$	$4.1 \cdot 10^6$	$2.0 \cdot 10^8$	$6.9 \cdot 10^6$	$-8.5 \cdot 10^6$

Table 7: The starting, final and difference in volume (in m^3) of all the elements in the 6-element simulation with 8 mm/year sea level rise

In the simulation with 8 mm/year sea level rise, almost all elements start to act as would

be expected. Channels are getting larger, flats and the delta are getting smaller and all are importing sediment to compensate for the extra water that is getting into the system. The only element for which this is not the case is the western flat, which still grows a little bit because of a large growth in the first few decades of the simulation. In total the basin loses $2.8 \cdot 10^8$ m^3 of sediment. The total increase in water volume due to sea level rise is $11 \cdot 10^8$, the total import of sediment is $8.1 \cdot 10^8$

6.2 10 element model

The results given by the modelling described in subsection 5.2, using ten elements, are presented in this subsection. The situations without sea level rise and with 2 mm/year and 8 mm/year sea level rise are examined, as stated in the introduction of this section. The results for 4 and 6 mm/year sea level rise can be found in Appendix B.

No sea level rise

First the case without sea level rise is investigated. The comparison is shown in figure 32.

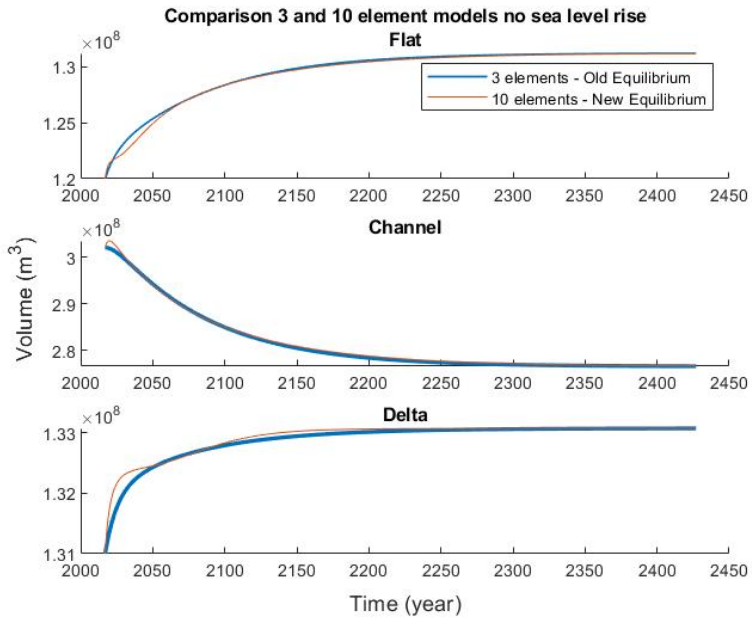

Figure 32: A comparison between the original 3 element and new 10 element model

As can been seen in the figure, the trajectory during the timeline is not perfectly represented by the model. The resulting equilibria, on the other hand, are very well represented by the model. The timescales of the original model and the 10-element model are very similar, but the spin up in the 10-element model still shows some differences with respect to the 3-element model. This is something that could be looked into in further research.

The blue lines in figure 33 and table 8 show the changes in channel volume for the different elements in the 10-element model without sea level rise. If looked into the local differences in between the different channel elements, some things stand out. Firstly, while the channels are decreasing in size overall and the western and far eastern elements follow this trend, the mid channel element is increasing in size substantially. This trend is opposite to the rest of

the basin. The changes in the first bifurcation channel are relatively small, with respect to the other channels. This element being the only other channel element which increases in size.

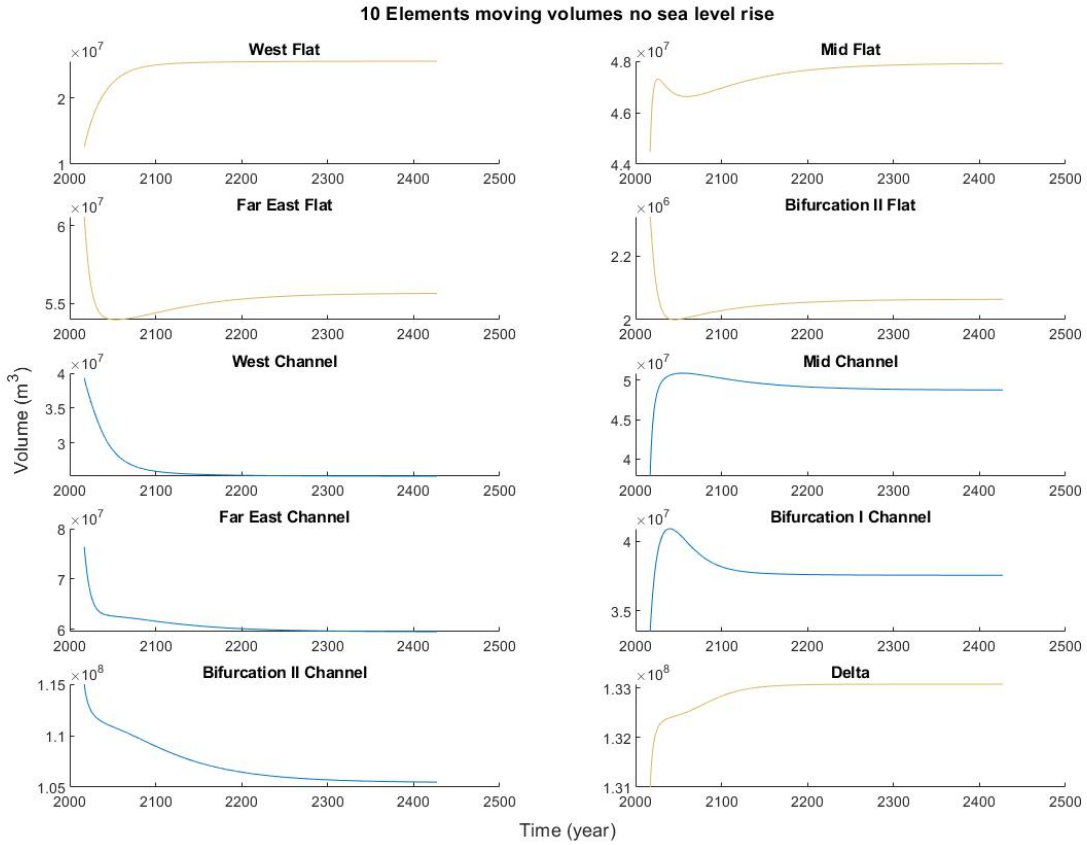

Figure 33: The change in volume of all elements in the 10-element model without sea level rise. Water volumes are blue and sand volumes are yellow.

If table 8 is compared to table 3 a few pages back, the thing that is most remarkable is that, while the entire eastern element in the 6-element model is getting smaller, this is not the case for all the subbasins within the eastern element. While sedimentation also occurs in the second bifurcation and the far eastern part of the basin, the mid channels are actually eroding. Furthermore, there is more sedimentation in the far eastern channel in the 10-element model than in its 'parent' east channel element in the 6-element model.

	Channels				
	West	*Mid*	*Far East*	*Bifurcation I*	*Bifurcation II*
Begin	$3.9 \cdot 10^7$	$3.8 \cdot 10^7$	$7.6 \cdot 10^7$	$3.4 \cdot 10^7$	$1.2 \cdot 10^8$
End	$2.5 \cdot 10^7$	$4.9 \cdot 10^7$	$6.0 \cdot 10^7$	$3.8 \cdot 10^7$	$1.1 \cdot 10^8$
Difference	$-1.4 \cdot 10^7$	$1.1 \cdot 10^7$	$-1.7 \cdot 10^7$	$4.1 \cdot 10^6$	$-9.5 \cdot 10^6$

Table 8: The starting, final and difference in volume (in m^3) of all the channels in the 10-element simulation without sea level rise

The changes in flat volume for the 10-element model without sea level rise can be found in most of the yellow lines in figure 33 and table 9. The increase in flat volume for the entire basin is

mainly due to the increase in the western flat. The other elements have a smaller contribution to the total basin, the far east and bifurcation flats even decrease in volume. If looked into the differences between tables 3 and 9, it shows that while the eastern element in table 3 shows very little change, the changes in two of the sub areas of this eastern element in 9 are actually larger than the changes in its 'parent' element.

	Flats				**Delta**
	West	*Mid*	*Far East*	*Bifurcation II*	
Begin	$1.3 \cdot 10^7$	$4.4 \cdot 10^7$	$6.1 \cdot 10^7$	$2.3 \cdot 10^6$	$1.3 \cdot 10^8$
End	$2.6 \cdot 10^7$	$4.8 \cdot 10^7$	$5.6 \cdot 10^7$	$2.1 \cdot 10^6$	$1.3 \cdot 10^8$
Difference	$1.3 \cdot 10^7$	$3.4 \cdot 10^6$	$-4.9 \cdot 10^6$	$-2.6 \cdot 10^5$	$2.1 \cdot 10^6$

Table 9: The starting, final and difference in volume (in m^3) of all the flats and the delta in the 10-element simulation without sea level rise

If looked at the general trends in the different parts of the basin, the western part imports a lot of sediment to reduce the channel size and increase the flat size. In the mid part the excess sediment that originates from the increase in channel volume partly ends up in the mid flats and partly elsewhere. The far eastern part has shrinking flats that contribute to the decrease in channel volume, but some sediment is imported from the rest of the basin. The basin exports a total of $3.9 \cdot 10^7$ m^3 sediment.

2 mm sea level rise per year

The 10-element model is subjected to the same sea level rise scenarios as the 6-element model. The 2 mm/year scenario as a representative of the current situation and the 8 mm/year scenario as a representative of the situation in 2050.

In the case without sea level rise a static equilibrium is reached. Because of the sea level rise in this simulation, a dynamic equilibrium is reached. The horizontal exchange comes into play in this dynamic equilibrium. The dynamic equilibrium in these simulations with sea level rise are quite sensitive to changes in the horizontal exchange. A measure of the fit of the calibration is the percentual difference in between the original and the 10-element model. As shown in figure 34 and table 10, the difference in the morphological equilibria of the 3 and 10 element models are quite substantial. There is a difference in the trajectory as well as the resulting ultimate dynamic equilibrium. Future research into the model and the horizontal exchange should be conducted to improve this.

	Flats	**Channels**	**Delta**
Final moving value 3EM	$1.2 \cdot 10^8$	$3.1 \cdot 10^8$	$1.3 \cdot 10^8$
Final moving value 10EM	$1.2 \cdot 10^8$	$3.2 \cdot 10^8$	$1.3 \cdot 10^8$
Difference	$-2.1 \cdot 10^6$	$3.7 \cdot 10^6$	$7.3 \cdot 10^3$
Percentual difference	-1.8%	1.2%	0.56%

Table 10: Comparison of the equilibrium volumes between the original model and the 10-element model for 2 mm/year sea level rise. All the values except from the percentages are in m^3.

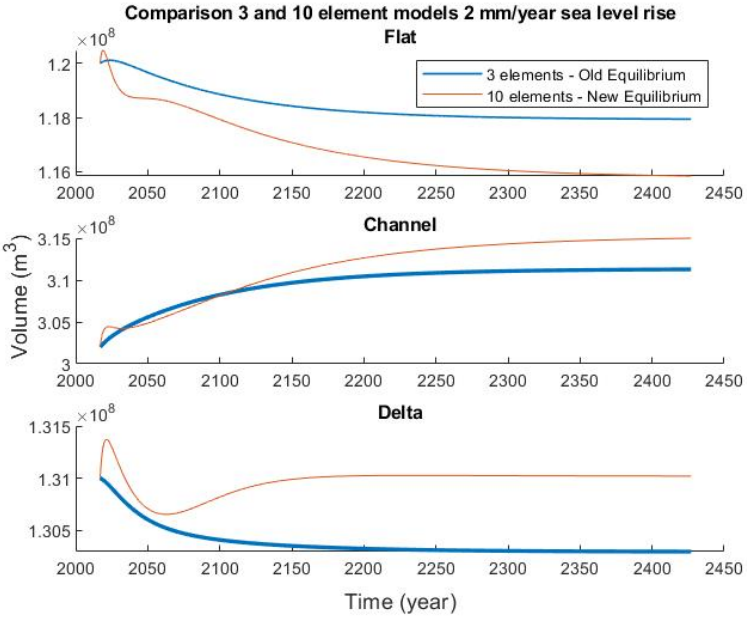

Figure 34: A comparison between the original 3 element and new 10 element model under 2 mm/year sea level rise

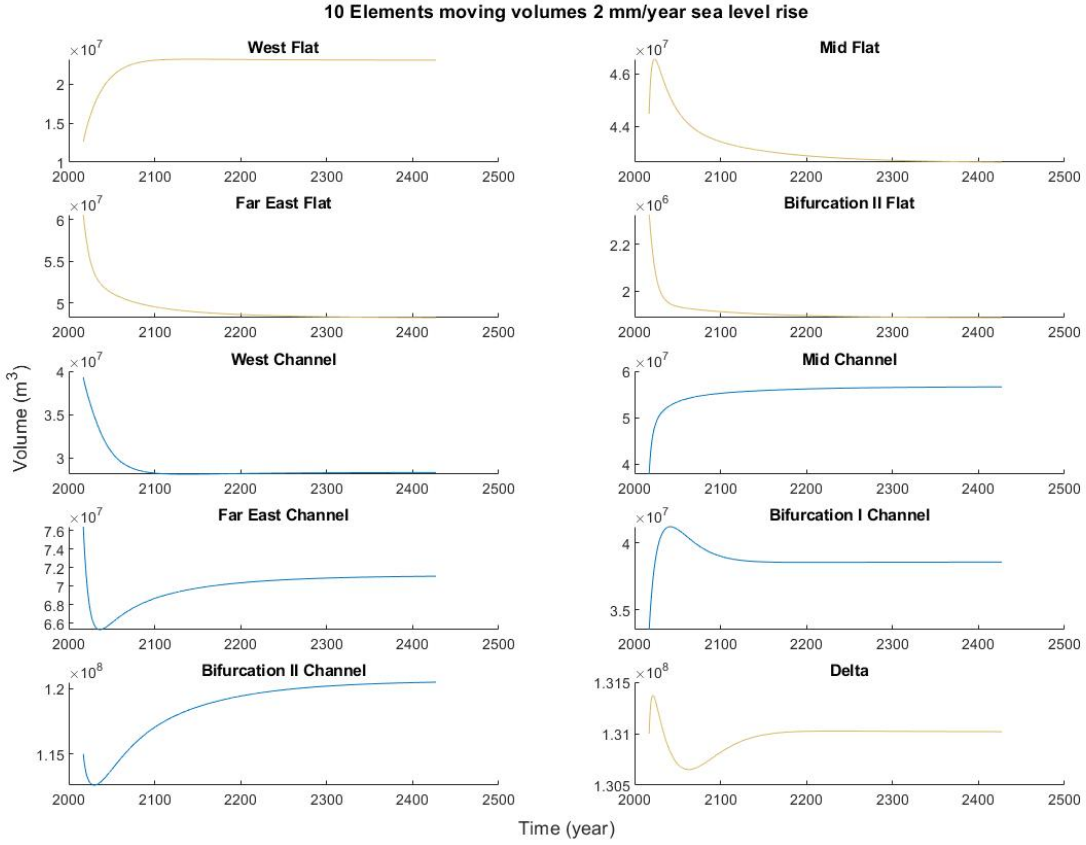

Figure 35: The change in volume of all elements in the 10-element model under 2 mm/year sea level rise. Water volumes are blue and sand volumes are yellow.

This simulation is also used to look into the individual elements. The results of all the elements are shown in figure 35 and tables 11 and 12. The blue lines in figure 35 and table 11 show the changes in channel volume. The general tendencies are similar to the model without sea level rise, except for the second bifurcation, which is increasing in volume instead of decreasing. The global increase of channel volume is mainly due to the mid channel, but both bifurcation channel elements do have a contribution as well. The west channel element decreases in volume substantially and the far east channel a bit.

	Channels				
	West	*Mid*	*Far East*	*Bifurcation I*	*Bifurcation II*
Begin	3.9 $\cdot 10^7$	3.8 $\cdot 10^7$	7.6 $\cdot 10^7$	3.4 $\cdot 10^7$	1.2 $\cdot 10^8$
End	2.8 $\cdot 10^7$	5.7 $\cdot 10^7$	7.1 $\cdot 10^7$	3.9 $\cdot 10^7$	1.2 $\cdot 10^8$
Difference	-1.1 $\cdot 10^7$	1.9 $\cdot 10^7$	-5.3 $\cdot 10^6$	5.1 $\cdot 10^6$	5.5 $\cdot 10^6$

Table 11: The starting, final and difference (in m^3) in volume of all the channels in the 10-element simulation with 2 mm/year sea level rise

The behaviour of the flats in the simulation with 2 mm/year sea level rise are shown in figure 35 and table 12. Most of the flats also show similar tendencies compared to the case without sea level rise in table 9. The mid flat is the only one that decreases in volume instead of increases, but in both models, it has a small contribution, compared to other elements. The contribution of the far east flat element is larger in this simulation than it was without sea level rise. The differences in the mid and far east elements are mostly responsible for the decrease in volume of the flats globally in the basin.

	Flats				**Delta**
	West	*Mid*	*Far East*	*Bifurcation II*	
Begin	1.3 $\cdot 10^7$	4.4 $\cdot 10^7$	6.1 $\cdot 10^7$	2.3 $\cdot 10^6$	1.3 $\cdot 10^8$
End	2.3 $\cdot 10^7$	4.3 $\cdot 10^7$	4.8 $\cdot 10^7$	1.9 $\cdot 10^6$	1.3 $\cdot 10^8$
Difference	1.0 $\cdot 10^7$	-1.9 $\cdot 10^6$	-1.2 $\cdot 10^7$	-4.4 $\cdot 10^5$	1.9 $\cdot 10^4$

Table 12: The starting, final and difference in volume (in m^3) of all the flats and the delta in the 10-element simulation with 2 mm/year sea level rise

The general trends in the basin are quite interesting. With no sediment transport, an increase of volume in the channels and a decrease of volume in the flats would have been expected. In the western part of the basin the channels decrease in volume as much as the flats increase, a lot of sediment import is taking place in this area. In the mid element part of the basin the channels increase in volume substantially combined with the small increase in flat volume, this is very typical for a basin that encounters sea level rise. In the far eastern part of the basin, the flats decrease in size substantially and the channels decrease in size a little bit. In the second bifurcation the channel increases and the flat decreases in size, the influence of sea level rise is clear in this part of the basin. The total basin loses $1.7 \cdot 10^7$ m^3 sediment. This is not an actual loss, but the result of sea level rise encountered by an import of sediment. Ass the sea level rises, flats decrease in size and channels increase in size, as former flat area becomes a part of a channel or channels get deeper. This effect is mitigated by the import of sediment. The extra volume of water of $2.7 \cdot 10^8$ due to sea level rise is almost compensated by a the total import of sediment over 400 years of $2.5 \cdot 10^8$ m^3.

8 mm sea level rise per year

Figure 36 and table 13 show that the general tendencies in the 8 mm/year sea level rise case are similar to the 3-element model. Especially the first few hundred years for the channel element and coming decades for the delta element show similar behaviour. The flat element differs earlier than the other elements. The timescale of the Delta element differs a lot in between the two models. In approximately 100 years an equilibrium is reached for the 10-element model, while the 3-element model is establishing a dynamic equilibrium over the entire time of the simulation. The 8 mm/year trajectory is a lot smoother than the 2 mm/year case. As this is a quite probable scenario for the coming years and the spatial differences in sedimentation and erosion are very important for the maintenance policy of Rijkswaterstaat, this model is very relevant.

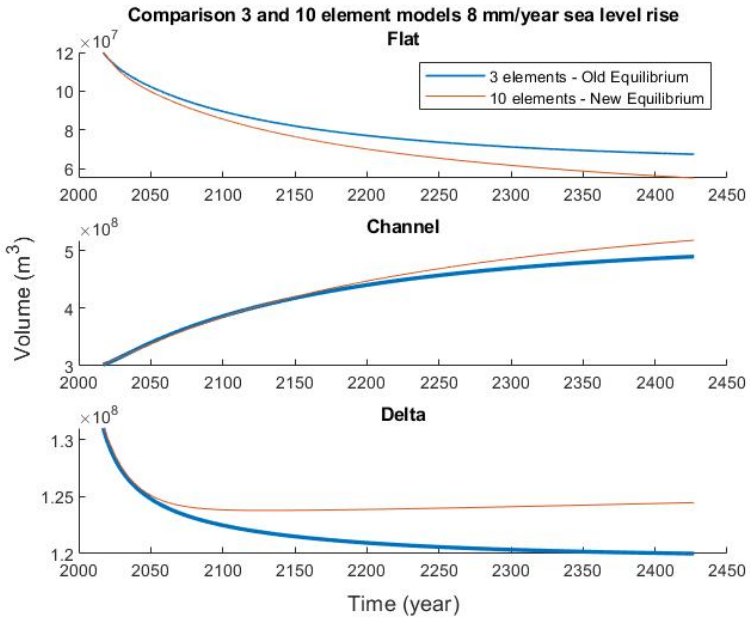

Figure 36: A comparison between the original 3 element and new 10 element model under 8 mm/year sea level rise

	Flats	**Channels**	**Delta**
Final moving value 3EM	$6.7 \cdot 10^7$	$4.9 \cdot 10^8$	$1.2 \cdot 10^8$
Final moving value 10EM	$5.5 \cdot 10^7$	$5.2 \cdot 10^8$	$1.2 \cdot 10^8$
Difference	$-1.2 \cdot 10^7$	$2.8 \cdot 10^7$	$4.5 \cdot 10^6$
Percentual difference	-18%	5.8%	3.7%

Table 13: Comparison of the equilibrium volumes between the original model and the 10-element model for 8 mm/year sea level rise. All the values except from the percentages are in m^3.

As is the case with the 6-element model, this case is also used to look into the spatial differences in the morphological responses of different elements. Figure 37 and tables 14 and 15 are used to look into these spatial differences.

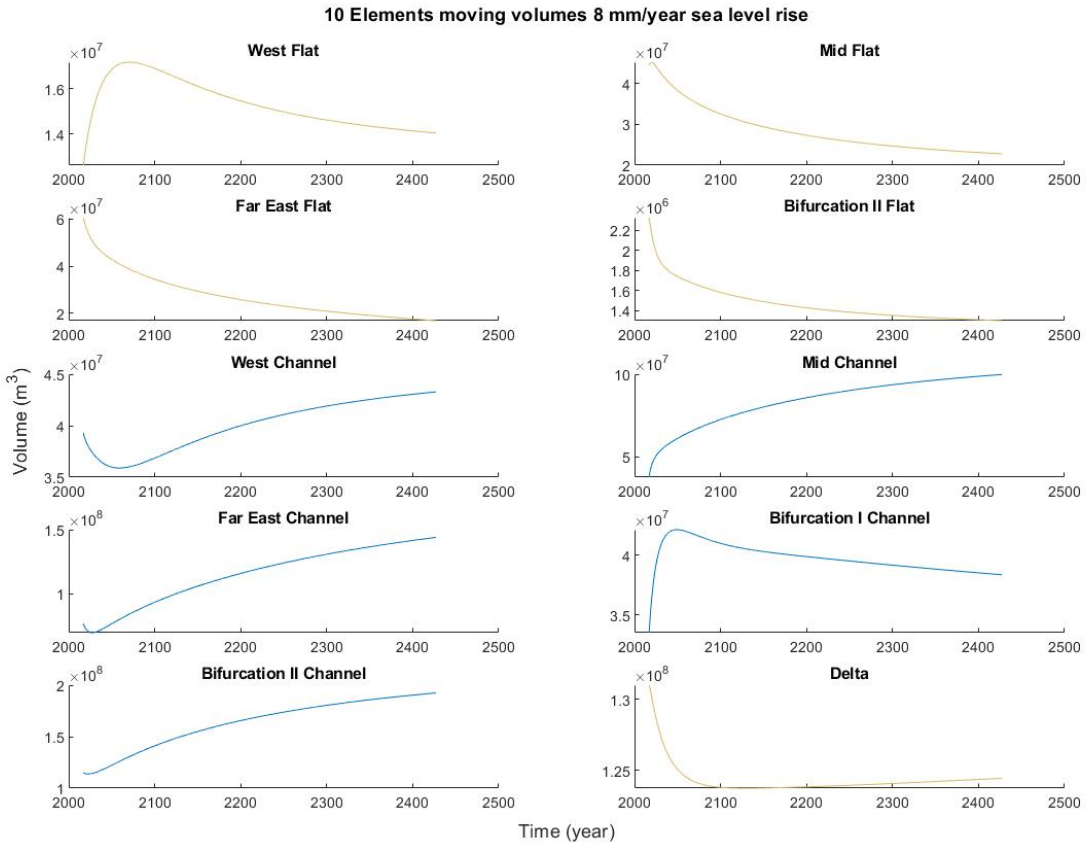

Figure 37: The change in volume of all elements in the 10-element model under 8 mm/year sea level rise. Water volumes are blue and sand volumes are yellow.

Figure 37 and table 14 go into the changes in the channels in the simulation with 10 elements and 8 mm/year sea level rise. Compared to the other sea level rise cases, it is quite significant that all the channels are increasing in volume over time. The biggest erosion takes place in the mid, far east and bifurcation elements. These elements together form the east element in the 6-element model, which also faces a lot of erosion in the simulation with 8 mm/year sea level rise. The west and bifurcation I elements show very comparable behaviour to their counterparts in the 6-element model.

	Channels				
	West	*Mid*	*Far East*	*Bifurcation I*	*Bifurcation II*
Begin	$3.9 \cdot 10^7$	$3.8 \cdot 10^7$	$7.6 \cdot 10^7$	$3.4 \cdot 10^7$	$1.2 \cdot 10^8$
End	$4.3 \cdot 10^7$	$1.0 \cdot 10^8$	$1.4 \cdot 10^8$	$3.8 \cdot 10^7$	$1.9 \cdot 10^8$
Difference	$4.0 \cdot 10^6$	$6.2 \cdot 10^7$	$6.8 \cdot 10^7$	$4.8 \cdot 10^6$	$7.7 \cdot 10^7$

Table 14: The starting, final and difference in volume (in m^3) of all the channels in the 10-element simulation with 8 mm/year sea level rise

With the flats there is less consensus. Figure 37 and table 15 show that the Western flat element is the only one that grows. It is the only region in the entire basin where sedimentation takes place. The other flats, all of the channels and the delta all encounter erosion, in order to accommodate for the higher sea level.

	Flats				**Delta**
	West	*Mid*	*Far East*	*Bifurcation II*	
Begin	$1.3 \cdot 10^7$	$4.4 \cdot 10^7$	$6.1 \cdot 10^7$	$2.3 \cdot 10^6$	$1.3 \cdot 10^8$
End	$1.4 \cdot 10^7$	$2.3 \cdot 10^7$	$1.7 \cdot 10^7$	$1.3 \cdot 10^6$	$1.2 \cdot 10^8$
Difference	$1.4 \cdot 10^6$	$-2.2 \cdot 10^7$	$-3.6 \cdot 10^7$	$-1.0 \cdot 10^6$	$-6.6 \cdot 10^6$

Table 15: The starting, final and difference in volume (in m^3) of all the flats and the delta in the 10-element simulation with 8 mm/year sea level rise

All elements but the western flat element sediment is not in the system anymore due to the sea level rise. The total 'loss' of sediment is $2.9 \cdot 10^8$ m^3. Due to the sea level rise $11 \cdot 10^8$ extra water is in the system. This is compensated by $8.0 \cdot 10^8$ m^3 import of sediment.

7 Discussion

The data analysis in this thesis shows that like in the case of entire basins, there is an equilibrium between the tidal prism and channel volume in subbasins. This relation shown in again equation 22. The equation differs a little bit from the original relation. As is described in subsection 3.6 this relation is valid for tidal subbasins with a tidal prism of more than 40 km^2, for basins smaller than this there is a lot more scatter.

$$V_C = 1.34 \cdot 10^{-7} \cdot P^{1.78} \tag{22}$$

It is very well possible to make a model out of a basin, using this equilibrium relationship for subbasins, as was shown in the modelling part of this thesis. Because of the static nature of the model and the dynamic behaviour of smaller subbasins in particular, there is a limit to the applicability of the model. The validity of the model has the same requirement as the limit that was used in deriving the equilibrium relation, the subbasins should be larger than 40 km^2. This is a very useful tool to determine the morphological response of the larger subbasins to sea level rise. The spatial differences between different parts of a basin can be investigated in this way.

From the modelling of various subbasins it's visible that the spatial differences in response to sea level rise are quite substantial. Over all the simulations it is visible that the highest sedimentation rates are in the western part of the basin. Here the flats grow in every single simulation and the channels only grow a little bit in the 8 mm/year simulation. Only after a few decades of simulation in the 8 mm/year cases the flats start to get smaller and the channels start to get larger. In the mid element a more expected trend is taking place. In both the 2 mm/year and the 8 mm/year cases the channels grow and the flats shrink, albeit the flats in the 2 mm/year simulation only after a few decades. In the static equilibrium case the flats grow here and the growth of the channel is smaller, compared to the cases with sea level rise. In the far east part of the basin both the channels and the flat shrink in the 2 mm/year sea level rise case, after a few decades of fast shrinkage, the channels start to grow in this part of the basin. As the sea level rise gets higher, the effect of growing channels and shrinking flats gets the upperhand over other processes taking place. The Bifurcation II channel behaves after a few decades in the 2 mm/year sea level rise case as is typical for a basin where the sea level rise becomes dominant.

The scatter in smaller basins also gives an interesting conclusion. In some of these basins, the channel volume drops significantly, while the tidal prism is not smaller. Relatively, in these small basins a smaller part of the tidal prism is transported through the channel and a larger part over the intertidal flats.

It is hard to investigate the sensitivity to the level of detail in modelling. While the method is able to investigate the spatial differences in the response, the level of detail cannot be set to a level that makes it possible to investigate this sensitivity. The 10-element model is already reaching the limits of the area sizes that can be modelled using this approach. It is therefore impossible to do an extensive analysis into the sensitivity of the subbasin area size.

In an ideal situation the comparison between the 3-element model and the 6 and 10-element models would have provided exactly the same morphological behaviour for equivalent elements. This is not the case. As the equilibria also differ from the 3-element model, a part of the solution probably lies in the values for the horizontal exchange. The somewhat course assumption is

made that the value for the dispersion coefficient does not change with changing elements. This value should be looked into more deeply in future research.

The tidal watersheds of the subbasin are based on a hydrodynamical simulation of the basin. As this is a snapshot and not the mean location of the tidal watershed over a larger period of time, some uncertainty comes from this approach. This is probably especially true for the smaller basins, as the area that is on the wrong side of the tidal watershed is probably relatively the largest with respect to the area of the basin in these basins. As these errors are probably very small, the bathymetry is also used in determining the tidal watershed, the number of small basins probably mediate the resulting equilibrium and the equilibrium is not valid for small basins anyway, the problems caused by this error are probably very small. Also, because the same watersheds are used for the analysis of the equilibrium and for the modelling, the error cancels itself out.

Another limitation lies in the cell size of the bathymetry data. The bathymetry data is not continuous but built up from cells with a mean depth for every cell. As is the case with the tidal watersheds, this error is also both in the data analysis and the modelling part of the thesis. This limitation is considered to be very small.

8 Conclusion

This study has showed that not only there is a relation between the tidal prism and channel volume in a subbasin, but it has also showed that we are able to make models of different levels of detail with the equilibria. There are still a few questions to be sort out, but the relevance of the applicability of a model which is able to describe the differences in morphological response of different areas within a basin over large timescales is out of the question. This approach has a broad range of applications in different tidal basins over the entire world.

The western part of the basins encounter relatively the most sedimentation. In the far eastern part the channels still shrink in the beginning under 2 mm/year sea level rise, but this changes after a few decades. The mid element has growing channels and shrinking flats already in the 2 mm/year sea level rise simulation, although the flats grow for the first few decades.

In a study of a tidal basin both the original method with only the morphological equilibrium for entire basins and new approach using both the equilibrium relation for entire basins as the one for channels in subbasins could be used. The advantage of using the original method is that it is less work to apply. The only subdivision that has to be made is in between the channel and flat elements, along the depth. Also, this method has been used frequently in the past and has therefore proven itself time and time again. The advantage of the new model is that if a more extensive study into a basin is conducted, spatial differences can be investigated. If this is part of the research question, the extra work provided by the identifying of more elements using hydrodynamical models or bathymetry data can be very well worth it.

Both hypotheses described at the beginning of this thesis can be accepted. First of all, the morphological equilibrium. There is a clear correlation between the tidal prism and channel volume in the subbasins of the Ameland Inlet. If this is the case for other inlets should still be confirmed. The morphological equilibrium has a little bit different shape as opposed to the one for entire basins and should not be applied to subbasins smaller than 40 km^2.

The second hypothesis is about the modelling. It is very well possible to model subbasins using a model that incorporates the morphological equilibrium for subbasins. It should be noted though that it can only be applied to other basins if more research is done about the equilibrium in these other basins, the situation in intertidal flats could be investigated and the horizontal exchange still has some uncertainty.

9 Recommendations for future work

A lot of subjects regarding the morphological equilibria of basins and subbasins can still be studied. Starting with a data analysis into the equilibrium volume of the tidal flats in a subbasin. The way this equilibrium volume is determined for the Asmita modelling exercise is exactly the same as was the case in the equilibrium for the flats of the entire basin. It is not entirely certain that the equilibrium for a total basin and a subbasin are exactly the same. Although in the case of channels in a subbasin, a larger percentage of the channels is divided into the bifurcation elements. This percentage is lower for tidal flats and therefore the difference will be less significant and this probably won't change the outcome completely, though it is a good step in improving the model.

The approach used in this thesis is not able to determine which part of the is most prone to drowning. In order to do this, model enhancements should be made. Different sediment particle size fractions play an important role in this. As sand is imported via the tidal inlet and concentrations of suspended sediment are the highest in the ends of the basin, the middle part should be most prone to drowning (Wang et al., 2018). In order to investigate this, the different sediment sizes should be added to the model.

Another step which could be taken is to try to model a different basin using historical data. By comparing the outcome of the model with the real-world changes in a basin, a lot can be learned about the performance and applicability of the model.

It would also be interesting to try to use the model in a modelling exercise in which other disturbances are present than sea level rise. If the model could be applied to investigate the consequences of a closure, nourishments or other interventions in a basin, this would be very valuable. It should be kept in mind though, that the applicability of the model stops at a certain scale. Larger interventions could probably be investigated with the model easily, especially closures would be interesting to study using the model. For nourishments our other smaller interventions it's probably harder to investigate them using the model.

A last very important step in enhancing the model would be studying the values for the dispersion coefficiente. In my thesis these values were assumed to be constant, if only part of a subbasin was examined. But the scale of the tidal flow velocity (u) and the hydraulic water depth (H) could differ a little bit, influencing the dispersion coefficient, horizontal exchange and therefore the transport inbetween elements.

At some point in time it might, unfortunately, be necessary to investigate the effects of faster sea level rise simulations.

References

Cleveringa, J. and Oost, A. P. (1999). The fractal geometry of tidal-channel systems in the dutch wadden sea. *Geologie en Mijnbouw*, 78(1):21–30.

Elias, E. (2019). Een actuele sedimentbalans van de waddenzee.

Elias, E., Stive, M., Bonekamp, H., and Cleveringa, J. (2003). Tidal inlet dynamics in response to human intervention. *Coastal engineering journal*, 45(04):629–658.

Elias, E., Van der Spek, A., Wang, Z. B., and De Ronde, J. (2012). Morphodynamic development and sediment budget of the dutch wadden sea over the last century. *Netherlands Journal of Geosciences*, 91(3):293–310.

Elias, E. and van der Spek, A. J. (2017). Dynamic preservation of texel inlet, the netherlands: understanding the interaction of an ebb-tidal delta with its adjacent coast. *Netherlands Journal of Geosciences*, 96(4):293–317.

Eysink, W. (1991). Morphologic response of tidal basins to changes: The dutch coast: Paper no. 8. In *Coastal Engineering 1990*, pages 1948–1961.

Eysink, W. (1992). *Impact of sea level rise on the morphology of the Wadden Sea in the scope of its ecological function*. Delft Hydraulics.

Kragtwijk, N., Zitman, T., Stive, M., and Wang, Z. (2004). Morphological response of tidal basins to human interventions. *Coastal engineering*, 51(3):207–221.

Lodder, Q. J., Wang, Z. B., Elias, E., van der Spek, A. J., de Looff, H., and Townend, I. H. (2019). Future response of the wadden sea tidal basins to relative sea-level rise—an aggregated modelling approach. *Water*, 11(10):2198.

Oost, A. P. (1995). *Dynamics and sedimentary developments of the Dutch Wadden Sea with a special emphasis on the Frisian Inlet: a study of the barrier islands, ebb-tidal deltas, inlets and drainage basins*. Faculteit Aardwetenschappen.

Stive, M. J. and Wang, Z. (2003). Morphodynamic modeling of tidal basins and coastal inlets. In *Elsevier oceanography series*, volume 67, pages 367–392. Elsevier.

Townend, I., Wang, Z. B., Stive, M., and Zhou, Z. (2016). Development and extension of an aggregated scale model: Part 1–background to asmita. *China Ocean Engineering*, 30(4):483–504.

Van Goor, M., Zitman, T., Wang, Z., and Stive, M. (2003). Impact of sea-level rise on the morphological equilibrium state of tidal inlets. *Marine Geology*, 202(3-4):211–227.

Wang, Z., Vroom, J., van Prooijen, B. C., Labeur, R. J., Stive, M. J., and Hansen, M. (2011). Development of tidal watersheds in the wadden sea. In *RCEM 2011: Proceedings of the 7th IAHR Symposium of River, Coastal and Estuarine Morphodynamics, Beijing, China, 6-8 September 2011*. Citeseer.

Wang, Z. B., De Vriend, H. J., Stive, M. J., Townend, I. H., Dohmen-Jansen, C., and Hulscher, S. (2008). On the parameter setting of semi-empirical long-term morphological models for estuaries and tidal lagoons.

Wang, Z. B., Elias, E., van der Spek, A. J., and Lodder, Q. J. (2018). Sediment budget and

morphological development of the dutch wadden sea: impact of accelerated sea-level rise and subsidence until 2100. *Netherlands Journal of Geosciences*, 97(3):183–214.

A 6 element figures 4 and 6 mm/year sea level rise

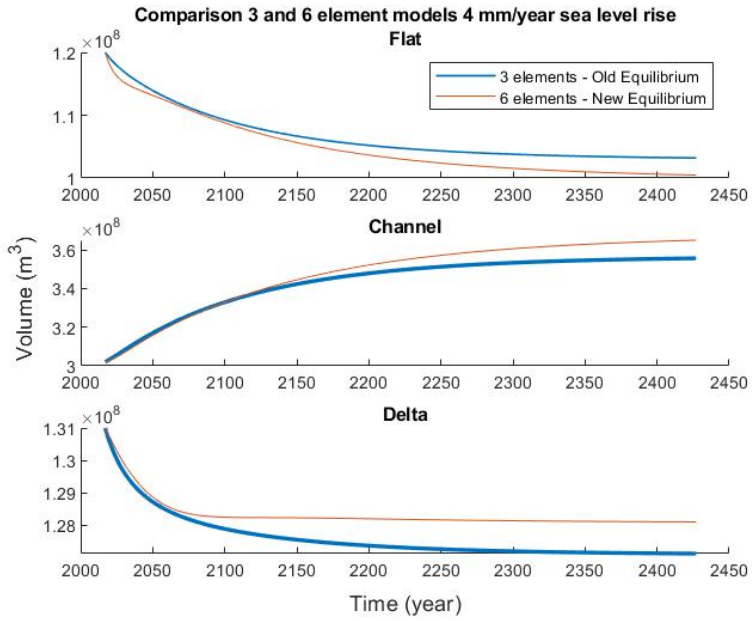

Figure 38: A comparison between the original 3 element and new 6 element model under 4 mm/year sea level rise

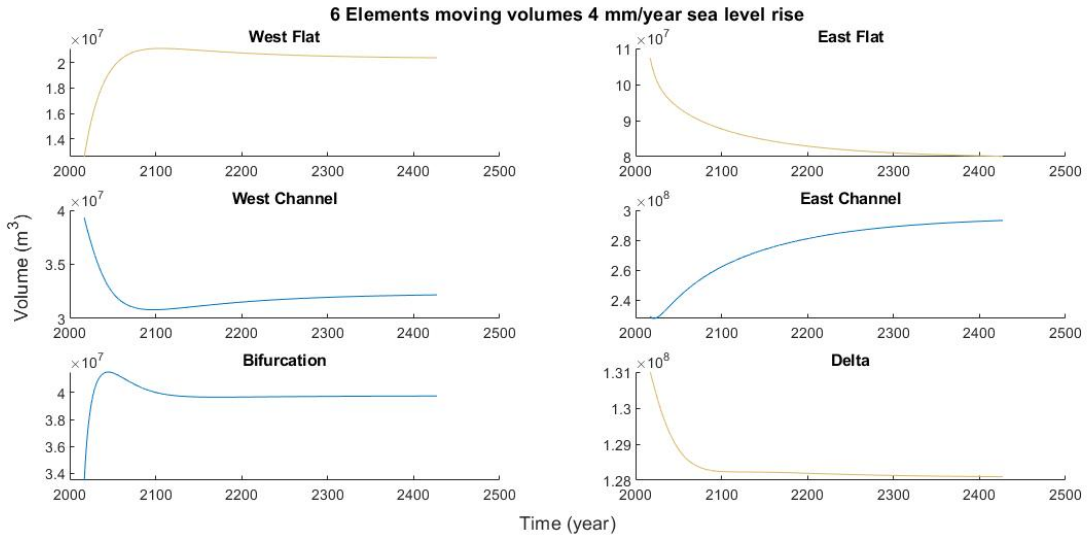

Figure 39: The change in volume of all elements in the 6 element model under 4 mm/year sea level rise. Water volumes are blue and sand volumes are yellow.

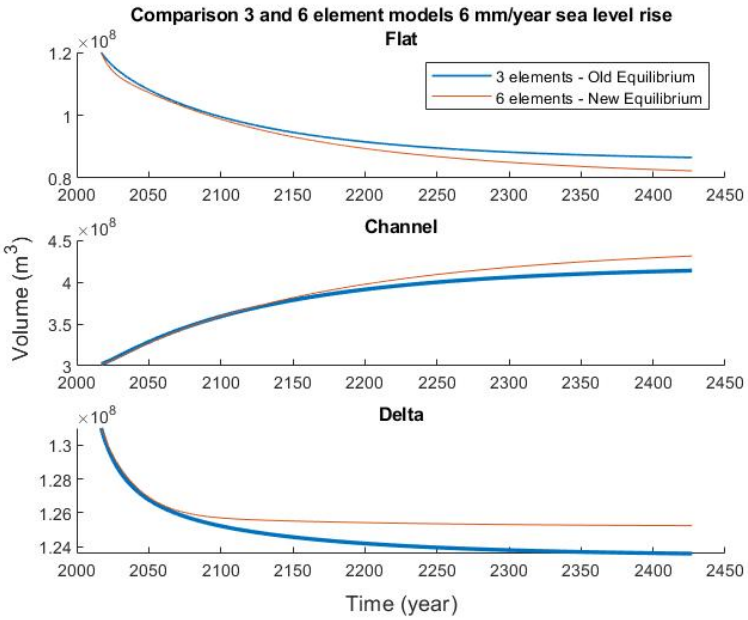

Figure 40: A comparison between the original 3 element and new 6 element model under 6 mm/year sea level rise

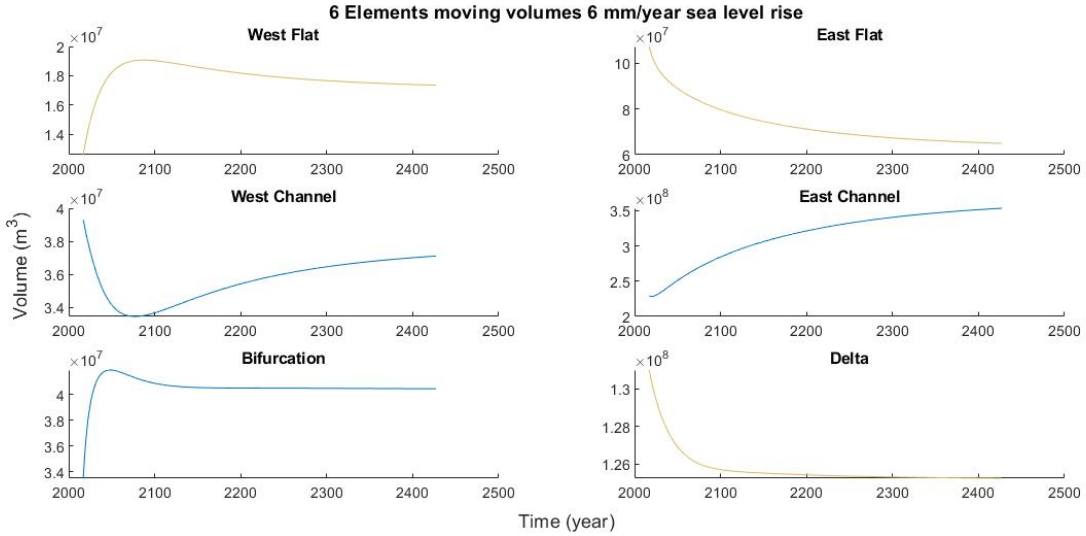

Figure 41: The change in volume of all elements in the 6 element model under 6 mm/year sea level rise. Water volumes are blue and sand volumes are yellow.

B 10 element figures 4 and 6 mm/year sea level rise

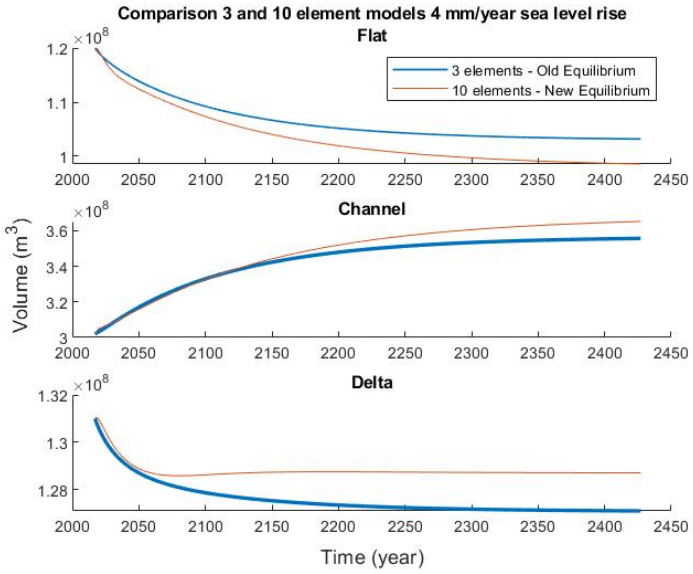

Figure 42: A comparison between the original 3 element and new 10 element model under 4 mm/year sea level rise

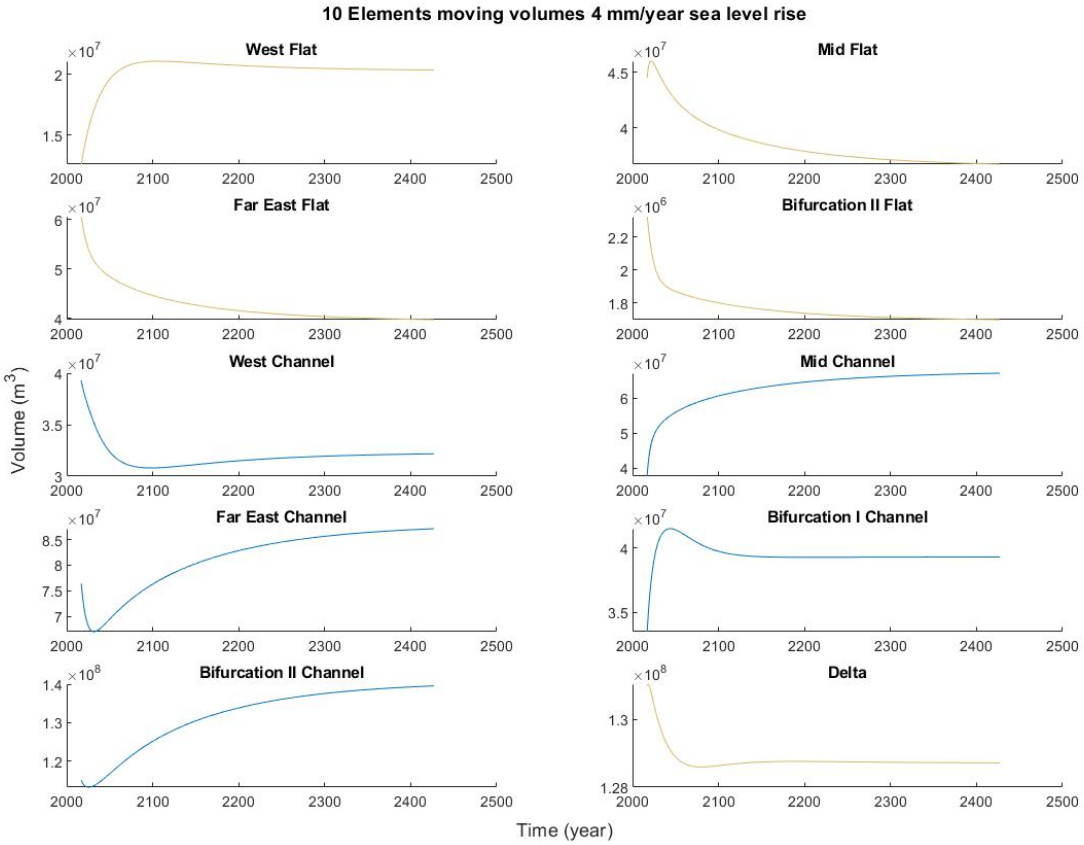

Figure 43: The change in volume of all elements in the 10 element model under 4 mm/year sea level rise. Water volumes are blue and sand volumes are yellow.

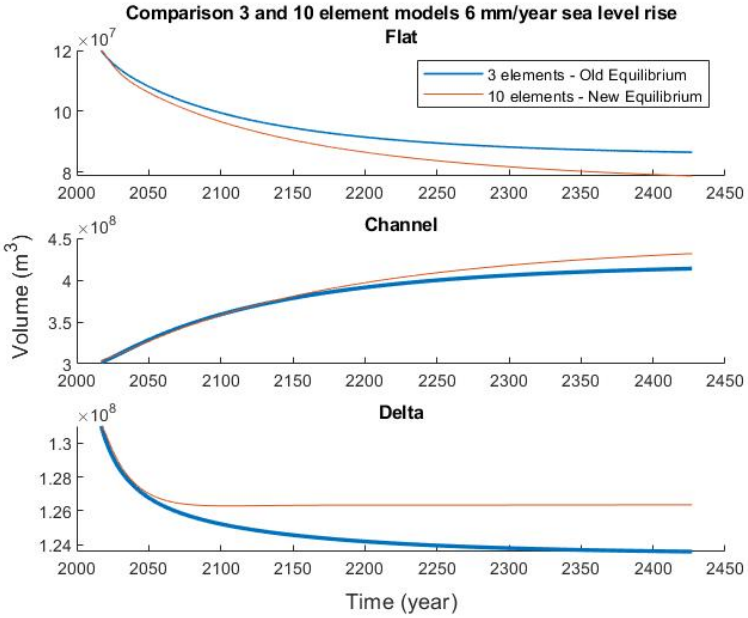

Figure 44: A comparison between the original 3 element and new 10 element model under 6 mm/year sea level rise

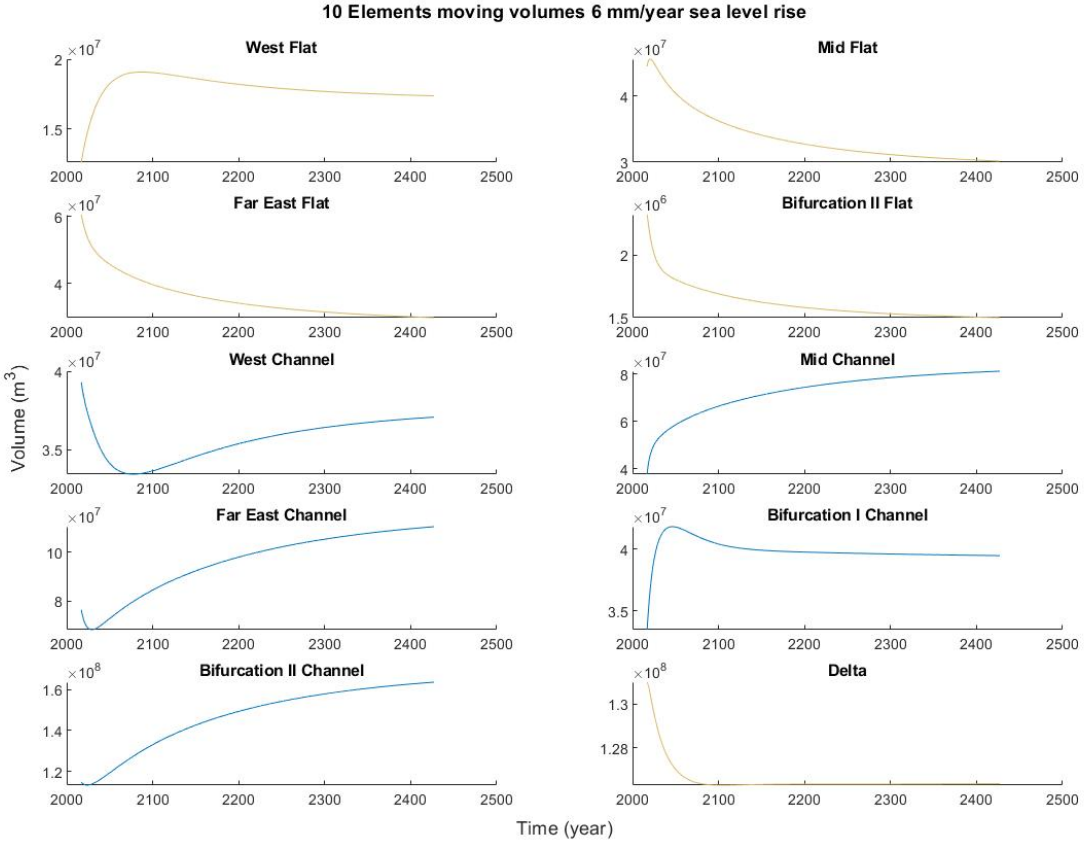

Figure 45: The change in volume of all elements in the 10 element model under 6 mm/year sea level rise. Water volumes are blue and sand volumes are yellow.

C 3 element matlab model

```
function [t,vm,ve,vt] = asmita_cf_codes_3E_OE(model,slr)
    %replicate the WZB fortran and Kragtwijk et al, 2004 versions of asmita
    % USAGE
    %   asmita_cf_codes(1,0.002)
    % INPUTS
    %   model - 1=WZB fortran; 2=Kragtwijk conc; 3=Kragtwijk conc [three methods give same result]
    %   slr - rate of sea level rise in m/year (optional, defaults to zero)
    % NOTE
    %   upper case variables are matrices, lower case scalar or vector
%     y2d = 360;                                %days in year - fortran code
    y2d = 365.2425;                             %days in year - ModelUI & asmitaOO
    d2s = 3600*24;                              %86400s in 1 day

    if nargin<2, slr = 0; end
    n = 3;                                      %no. of elements
    h = 2.15;                                   %tidal range (m)
    dt = 3;                                     %time step in days
    nt = (2*4*15600)/2.5;                               %number of time steps
%     nt = 1;

    %element properties 1=flat; 2=channel; 3=delta
    s = [1.78e8;9.83e7;7.47e7];                 %element plan area (m^2)
    v = [1.2e8;3.02e8;1.31e8];                  %element volume (m^3)
    cE = [2e-4;2e-4;2e-4];                      %equilibrium concentration (-)
    ws = [1e-4;5e-5;1e-5];                      %vertical exchange (m/s)

    mu  = [1; -1; 1];                           %element volume type (-)
    en = [2; 2; 2];                             %transport coefficient (-)
    nc0 = 1;                                    %number of external links
    cE0(1,:) = [3,2e-4];                        %id of element, external equilibrium concentration
    delta0(1,:) = [3,1500];                     %id of element to outside, horizontal exchange rate (m^3/s)
    nci = 2;                                    %number of internal
```

```
        links
33      deltai(1,:) = [1,2,1000];                    %i,j of elements,
        horizontal exchange rate (m^3/s)
34      deltai(2,:) = [2,3,1500];                    %i,j of elements,
        horizontal exchange rate (m^3/s)
35      alpha = [1.312e8; 1.0241e-5; 2.9216e-3]; %equilibrium scale
        coefficients
36      beta = [0.0; 1.55; 1.23];                    %equilibrium shape
        coefficients
37      %slr                                         %rate of sea level
        rise m/yr
38      t = ([0,1:nt]*dt/y2d)';                      %time in years
39      dslr = slr/y2d*dt;                           %slr/dt (m)
40
41      w = ws*d2s;                                  %vertical exchange in
        days
42      dExt = zeros(length(n),1);   c0 = dExt;      %external exchange
43      delta = zeros(n);                            %horizontal exchange
        matrix
44      for j=1:nc0                                  %assign external
        exchanges
45          c0(cE0(j,1),1) = cE0(j,2);
46          dExt(delta0(j,1),1) = delta0(j,2);
47      end
48      %
49      for j=1:nci                                  %assign internal
        exchanges
50          delta(deltai(j,1),deltai(j,2)) = deltai(j,3);
51      end
52
53      switch model
54          case 1
55              model = 'WZB fortran';
56              asmita_fortran();
57          case {2,3}
58              asmita_kragtwijk();
59      end
60      vm = vm';   ve = ve';    vt = vt';           %transpose output
        arrays
61  %     plotVolumes(t,vm,ve,vt,model)              %plot results
62
63  %-nested function
    ------------------------------------------------------------------
64      function asmita_kragtwijk()
65          mu = -mu;                              %Kragtwijk uses
            opposite convention
66          delta = delta+delta';
67          D = -delta;
```

```
68          for j=1:n
69              D(j,j) = sum(delta(j,:))+dExt(j);
70          end
71          Amat = D*d2s;                          %horizontal exchange
                matrix per day
72          Amat = Amat+diag(w.*s);                %LHS matrix (D+W)
73          dExt = dExt*d2s;
74          %--------------------------------------%solve concentration
                as per WZB fortran
75          if model==2
76              [L,U] = lu(Amat);                  %LU factorization of
                    dispersion matrix
77              vm = zeros(n,nt);
78              vm(:,1) = v;    [ve(:,1),vt(1,1)] = mkve(h,s,v,alpha,beta
                    );
79              for jt=2:nt+1
80                  vmjt = vm(:,jt-1);
81                  [vejt,vtjt] = mkve(h,s,vmjt,alpha,beta); %
                        equilibrium volume
82                  ce = cE.*(vejt./vmjt).^(mu.*en);  %local equilibrium
                         concentration
83                  rhs = dExt.*c0+w.*s.*ce;          %rhs of
                        conservation equation
84                  c = U\(L\rhs);                    %solve A.x = b
                        where A=amat and b=rhs
85                                                    %note: no
                                                          different to c
                                                         = amat\rhs;
86                  dvm = mu.*s.*dslr;                %change in water
                        volume due to slr
87                  vmjt = vmjt+w.*s.*mu.*(ce-c)*dt+dvm;
88                  vmjt(vmjt<0) = 0;                 %trap negative
                        volumes
89                  vm(:,jt) = vmjt;                  %moving volume
90                  ve(:,jt) = vejt;                  %equilibrium
                        volume
91                  vt(1,jt) = vtjt;                  %tidal prism
92              end
93              model = 'Kragtwijk using conc';
94          %--------------------------------------%solve using B and
                d explicit solution
95          else
96              D = D*d2s;                         %horizontal exchange
                    matrix per day
97              W = diag(w.*s);
98              vm(:,1) = v;    [ve(:,1),vt(1,1)] = mkve(h,s,v,alpha,beta
                    );
99              for jt=2:nt+1
```

```
100                 vmjt = vm(:,jt-1);
101                 [vejt,vtjt] = mkve(h,s,vmjt,alpha,beta);  %
                        equilibrium volume
102                 gamma = (vejt./vmjt).^(mu.*en);     %local equilibrium
                        ratio
103                 B = diag(cE.*mu)*W*(eye(3)-(D+W)\W);
104                 if sum(W)==0      %used to test code - only change is
                        water level
105                     dd = w;
106                 else
107                     dd = diag(cE.*mu)*W*((D+W)\dExt);
108                 end
109                 dvm = mu.*s.*dslr;                      %change in water
                        volume due to slr
110                 vmjt = vmjt+(B*gamma-dd)*dt+dvm;     %Eq.17 and !8,
                        Kragtwijk etal, 2004
111                 vmjt(vmjt<0) = 0;                       %trap negative
                        volumes
112                 vm(:,jt) = vmjt;                        %moving volume
113                 ve(:,jt) = vejt;                        %equilibrium
                        volume
114                 vt(1,jt) = vtjt;                        %tidal prism
115             end
116             model = 'Kragtwijk using B and d';
117         end
118     end
119 %-nested function
    ------------------------------------------------------------------
120     function asmita_fortran()
121         %solve concentration using matrix convention as per WZB
                fortran
122         delta = delta+delta';
123         D = delta;
124         for j=1:n
125             D(j,j) = -sum(delta(j,:))-dExt(j);
126         end
127         Amat = D*d2s;                               %horizontal exchange
                matrix per day
128         Amat = Amat-diag(w.*s);                     %LHS matrix (D+W)
129         dExt = dExt*d2s;
130
131         [L,U] = lu(Amat);                           %LU factorization of
                dispersion matrix
132         vm = zeros(n,nt);
133         vm(:,1) = v;    [ve(:,1),vt(1,1)] = mkve(h,s,v,alpha,beta);
134         for jt=2:nt+1
135             vmjt = vm(:,jt-1);
136             [vejt,vtjt] = mkve(h,s,vmjt,alpha,beta); %equilibrium
```

```
                volume
137             ce = cE.*(vmjt./vejt).^(mu.*en);   %local equilibrium
                concentration
138             rhs = -dExt.*c0-w.*s.*ce;          %rhs of conservation
                equation
139             c = U\(L\rhs);                     %solve A.x = b where A
                =amat and b=rhs
140                                                %note: no different to
                                                       c = amat\rhs;
141             dvm = mu.*s.*dslr;                 %change in water
                volume due to slr
142             vmjt = vmjt+w.*s.*mu.*(c-ce)*dt-dvm;
143             vmjt(vmjt<0) = 0;                  %trap negative volumes
144             vm(:,jt) = vmjt;
145             ve(:,jt) = vejt;                   %equilibrium volume
146             vt(1,jt) = vtjt;                   %tidal prism
147         end
148     end
149 end
150 %%
151 function [ve,vt] = mkve(h,S,v,alpha,beta)
152     %define equilibrium volumes
153     sbasin = S(1)+S(2);          %plan area of basin (flat + channel)
154     vt = sbasin*h-v(1);          %tidal prism
155     ve = alpha.*vt.^beta;        %equilibrium volume
156 end
157 %%
```

D 6 element matlab model

```
function [t,vm,ve,vt] = asmita_cf_codes_6E_NE(model,slr)
    %replicate the WZB fortran and Kragtwijk et al, 2004 versions of asmita
    % USAGE
    % asmita_cf_codes(1,0.002)
    % INPUTS
    % model - 1=WZB fortran; 2=Kragtwijk conc; 3=Kragtwijk conc [three methods give same result]
    % slr - rate of sea level rise in m/year (optional, defaults to zero)
    % NOTE
    % upper case variables are matrices, lower case scalar or vector
    y2d = 365.2425;                                 %days in year - ModelUI & asmitaOO
    d2s = 3600*24;                                  %86400s in 1 day

    if nargin<2, slr = 0; end
    n = 6;                                          %no. of elements
    h = 2.15;                                       %tidal range (m)
    dt = 3;                                         %time step in days
    nt = (2*4*15600)/2.5;                           %number of time steps

    %element properties 1=West Flat; 2=East Flat; 3=West Channel;
    %4=East Channel; 5=Bifurcation ; 6=Delta
    s = [3.466e7;1.4334e8;2.59e7;6.74e7;5e6;7.47e7];        %element plan area (m^2);
    v = [1.2625e7;1.07375e8;3.93e7;2.292e8;3.35e7;1.31e8]; %element volume (m^3);
    cE = [2e-4;2e-4;2e-4;2e-4;2e-4;2e-4];   %equilibrium concentration (-)
    ws = [1e-4;1e-4;5e-5;5e-5;5e-5;1e-5];   %vertical exchange (m/s)
    mu  = [1;1; -1;-1;-1; 1];               %element volume type (-)
    en = [2; 2; 2; 2; 2; 2];                %transport coefficient (-)

    nc0 = 1;                                                    %number of external links
    cE0(1,:) = [6,2e-4];                    %id of element, external equilibrium concentration
    delta0(1,:) = [6,1500];                 %id of element to outside, horizontal exchange rate (m^3/s)
    nci = 5;                                %number of internal links
    deltai(1,:) = [1,3,214];                %i,j of elements, horizontal exchange rate (m^3/s)
    deltai(2,:) = [2,4,786];                %i,j of elements, horizontal exchange rate (m^3/s)
```

```
34      deltai(3,:) = [3,5,573];                    %i,j of elements,
           horizontal exchange rate (m^3/s)
35      deltai(4,:) = [4,5,1133];                   %i,j of elements,
           horizontal exchange rate (m^3/s)
36      deltai(5,:) = [5,6,3900];                   %i,j of elements,
           horizontal exchange rate (m^3/s)
37      alpha = [25547146; 105652854; 1.34e-7;1.34e-7; 1.0241e-5; 2.9216
           e-3]; %equilibrium scale coefficients
38      beta = [0;0; 1.78;1.78;1.55; 1.23];
                                                %equilibrium shape
           coefficients
39      t = ([0,1:nt]*dt/y2d)';                     %time in years
40      dslr = slr/y2d*dt;                          %slr/dt (m)
41
42      w = ws*d2s;                 %vertical exchange in days
43      dExt = zeros(length(n),1);
44      c0 = dExt;                  %external exchange
45      delta = zeros(n);           %horizontal exchange matrix
46      for j=1:nc0                 %assign external exchanges
47          c0(cE0(j,1),1) = cE0(j,2);
48          dExt(delta0(j,1),1) = delta0(j,2);
49      end
50      %
51      for j=1:nci                  %assign internal exchanges
52          delta(deltai(j,1),deltai(j,2)) = deltai(j,3);
53      end
54
55      switch model
56          case 1
57              model = 'WZB fortran';
58              asmita_fortran();
59          case {2,3}
60              asmita_kragtwijk();
61      end
62      vm = vm';   ve = ve';    vt = vt'; %transpose output arrays
63
64  %-nested function
    ------------------------------------------------------------------
65      function asmita_kragtwijk()
66          mu = -mu;             %Kragtwijk uses opposite convention
67          delta = delta+delta';
68          D = -delta;
69          for j=1:n
70              D(j,j) = sum(delta(j,:))+dExt(j);
71          end
72          Amat = D*d2s;         %horizontal exchange matrix per day
73          Amat = Amat+diag(w.*s);  %LHS matrix (D+W)
74          dExt = dExt*d2s;
```

```
75          %--------------------%solve concentration as per WZB fortran
76          if model==2
77              [L,U] = lu(Amat);       %LU factorization of dispersion
                    matrix
78              vm = zeros(n,nt);
79              vm(:,1) = v;    [ve(:,1),vt(1,1),vt1(1,1),vt2(1,1)] =
                    mkve(h,s,v,alpha,beta,n);
80              for jt=2:nt+1
81                  vmjt = vm(:,jt-1);
82                  [vejt,vtjt,vt1jt,vt2jt] = mkve(h,s,vmjt,alpha,beta,n
                        ); %equilibrium volume
83                  ce = cE.*(vejt./vmjt).^(mu.*en);  %local equilibrium
                         concentration
84                  rhs = dExt.*c0+w.*s.*ce;          %rhs of
                        conservation equation
85                  c = U\(L\rhs);      %solve A.x = b where A=amat and b
                        =rhs
86                                      %note: no different to c = amat\
                            rhs;
87                  dvm = mu.*s.*dslr; %change in water volume due to
                        slr
88                  vmjt = vmjt+w.*s.*mu.*(ce-c)*dt+dvm;
89                  vmjt(vmjt<0) = 0;           %trap negative volumes
90                  vm(:,jt) = vmjt;            %moving volume
91                  ve(:,jt) = vejt;            %equilibrium volume
92                  vt(1,jt) = vtjt;            %tidal prism
93                  vt1(1,jt) = vt1jt;
94                  vt2(1,jt) = vt2jt;
95              end
96              model = 'Kragtwijk using conc';
97          %--------------------%solve using B and d explicit solution
98          else
99              D = D*d2s;                              %horizontal exchange
                    matrix per day
100             W = diag(w.*s);
101             vm(:,1) = v;    [ve(:,1),vt(1,1),vt1(1,1),vt2(1,1)] =
                    mkve(h,s,v,alpha,beta,n);
102             for jt=2:nt+1
103                 vmjt = vm(:,jt-1);
104                 [vejt,vtjt,vt1jt,vt2jt] = mkve(h,s,vmjt,alpha,beta,n)
                        ; %equilibrium volume
105                 gamma = (vejt./vmjt).^(mu.*en);     %local equilibrium
                         ratio
106                 B = diag(cE.*mu)*W*(eye(n)-(D+W)\W);
107                 if sum(W)==0      %used to test code - only change is
                        water level
108                     dd = w;
109                 else
```

```
110                     dd = diag(cE.*mu)*W*((D+W)\dExt);
111                 end
112                 dvm = mu.*s.*dslr;                      %change in water
                        volume due to slr
113                 vmjt = vmjt+(B*gamma-dd)*dt+dvm;        %Eq.17 and !8,
                        Kragtwijk etal, 2004
114                 vmjt(vmjt<0) = 0;                       %trap negative volumes
115                 vm(:,jt) = vmjt;                        %moving volume
116                 ve(:,jt) = vejt;                        %equilibrium volume
117                 vt(1,jt) = vtjt;                        %tidal prism
118                 vt1(1,jt) = vt1jt;
119                 vt2(1,jt) = vt2jt;
120             end
121             model = 'Kragtwijk using B and d';
122         end
123     end
124 %-nested function
    ------------------------------------------------------------------------
125     function asmita_fortran()
126         %solve concentration using matrix convention as per WZB
                fortran
127         delta = delta+delta';
128         D = delta;
129         for j=1:n
130             D(j,j) = -sum(delta(j,:))-dExt(j);
131         end
132         Amat = D*d2s;                   %horizontal exchange matrix per day
133         Amat = Amat-diag(w.*s);         %LHS matrix (D+W)
134         dExt = dExt*d2s;
135
136         [L,U] = lu(Amat);               %LU factorization of dispersion
                matrix
137         vm = zeros(n,nt);
138         vm(:,1) = v;    [ve(:,1),vt(1,1),vt1(1,1),vt2(1,1)] = mkve(h,
                s,v,alpha,beta,n);
139         for jt=2:nt+1
140             vmjt = vm(:,jt-1);
141             [vejt,vtjt,vt1jt,vt2jt] = mkve(h,s,vmjt,alpha,beta, n);
                  %equilibrium volume
142             ce = cE.*(vmjt./vejt).^(mu.*en);  %local equilibrium
                    concentration
143             rhs = -dExt.*c0-w.*s.*ce; %rhs of conservation equation
144             c = U\(L\rhs);                  %solve A.x = b where A=amat
                    and b=rhs
145             %note: no different to c = amat\rhs;
146             dvm = mu.*s.*dslr;              %change in water volume due to
                     slr
147             vmjt = vmjt+w.*s.*mu.*(c-ce)*dt-dvm;
```

```
148                 vmjt(vmjt<0) = 0;                   %trap negative volumes
149                 vm(:,jt) = vmjt;
150                 ve(:,jt) = vejt;                    %equilibrium volume
151                 vt(1,jt) = vtjt;                    %tidal prism
152                 vt1(1,jt) = vt1jt;
153                 vt2(1,jt) = vt2jt;
154             end
155         end
156 end
157 %%
158 function [ve,vt,vt1,vt2] = mkve(h,S,v,alpha,beta,n)
159     %define equilibrium volumes
160     sbasin1 = S(1)+S(3);            %plan area of subbasin (west) (flat
            + channel)
161     sbasin2 = S(2)+S(4);            %plan area of subbasin (east) (flat
            + channel)
162     vt1 = sbasin1*h-v(1);           %tidal prism of subbasin west
163     vt2 = sbasin2*h-v(2);           %tidal prism of subbasin east
164     vt = vt1+vt2+(S(5)*h);          %tidal prism of basin
165     ve = zeros(n,1);
166     for i = 1:n
167         if i == 1 | i == 3
168             ve(i) = alpha(i)*(vt1^beta(i)); %equilibrium volume west
169         elseif i == 2| i == 4
170             ve(i) = alpha(i)*(vt2^beta(i)); %equilibrium volume east
171         elseif i == 5
172             vet = alpha(i)*(vt^beta(i));    %channel equilibrium
                    volume total
173             ve(i) = vet - ve(3) - ve(4);    %Delta channel
                    equilibrium volume
174         elseif i == 6
175             ve(i) = alpha(i)*(vt^beta(i));  %equilibrium volume
                    delta
176         end
177     end
178 end
179 %%
```

E 10 element matlab model

```
function [t,vm,ve,vt] = asmita_cf_codes_10E_NE(model,slr)
    %replicate the WZB fortran and Kragtwijk et al, 2004 versions of asmita
    % USAGE
    %   asmita_cf_codes(1,0.002)
    % INPUTS
    %   model - 1=WZB fortran; 2=Kragtwijk conc; 3=Kragtwijk conc [three methods give same result]
    %   slr - rate of sea level rise in m/year (optional, defaults to zero)
    % NOTE
    %   upper case variables are matrices, lower case scalar or vector
%     y2d = 360;                                  %days in year - fortran code
    y2d = 365.2425;                             %days in year - ModelUI & asmitaOO
    d2s = 3600*24;                              %86400s in 1 day

    if nargin<2, slr = 0; end
    n = 10;                                      %no. of elements
    h = 2.15;                                   %tidal range (m)
    dt = 3;                                     %time step in days
    nt = (2*4*15600)/2.5;                                %number of time steps
%     nt = 1;

    %element properties 1=West flat; 2=Mid Flat; 3=Far East Flat;
    %4=Bifurcation II Flat; 5=West Channel; 6=Mid Channel;
    %7=Far East Channel; 8=Bifurcation II Channel ;
    %9=Bifurcation I Channel; 10=Delta
    s = [3.466e7;6.502e7;7.552e7;2.8e6;2.59e7;2.77e7;2.92e7;1.05e7;5e6;7.47e7];%      %element plan area (m^2) [1.78e8;9.83e7;7.47e7];
    v = [1.2625e7;4.4475e7;6.0575e7;2.3250e6;3.93e7;3.78e7;7.64e7;1.15e8;3.35e7;1.31e8];%[      %element volume (m^3)1.2e8;3.02e8;1.31e8];
    cE = [2e-4;2e-4;2e-4;2e-4;2e-4;2e-4;2e-4;2e-4;2e-4;2e-4];
                                %equilibrium concentration (-)
    ws = [1e-4;1e-4;1e-4;1e-4;5e-5;5e-5;5e-5;5e-5;5e-5;1e-5];
                                %vertical exchange (m/s)

    mu  = [1;1;1;1; -1;-1;-1;-1;-1; 1];                                 % element volume type (-)
    en = [2; 2; 2; 2; 2; 2; 2; 2; 2; 2];                                % transport coefficient (-)
    nc0 = 1;                                    %number of external
```

```
    links
cE0(1,:) = [10,2e-4];                    %id of element,
    external equilibrium concentration
delta0(1,:) = [10,1500];                 %id of element to
    outside, horizontal exchange rate (m^3/s)
nci = 9;                                 %number of internal
    links
deltai(1,:) = [9,10,3900];               %i,j of elements,
    horizontal exchange rate (m^3/s)
deltai(2,:) = [9,5,573];                 %i,j of elements,
    horizontal exchange rate (m^3/s)
deltai(3,:) = [5,1,214];                 %i,j of elements,
    horizontal exchange rate (m^3/s)
deltai(4,:) = [9,8,1925];                %i,j of elements,
    horizontal exchange rate (m^3/s)
deltai(5,:) = [8,4,29];                  %i,j of elements,
    horizontal exchange rate (m^3/s)
deltai(6,:) = [8,7,731];                 %i,j of elements,
    horizontal exchange rate (m^3/s)
deltai(7,:) = [7,3,343];                 %i,j of elements,
    horizontal exchange rate (m^3/s)
deltai(8,:) = [8,6,1142];                %i,j of elements,
    horizontal exchange rate (m^3/s)
deltai(9,:) = [6,2,414];                 %i,j of elements,
    horizontal exchange rate (m^3/s)
alpha = [25547146; 47924854;55664180;2063820; 1.34e-7;1.34e
    -7;1.34e-7;1.34e-7; 1.0241e-5; 2.9216e-3]; %equilibrium scale
     coefficients
beta = [0;0;0;0;1.78;1.78;1.78;1.78;1.55;1.23];
    %equilibrium shape coefficients
%slr                                     %rate of sea level
    rise m/yr
t = ([0,1:nt]*dt/y2d)';                  %time in years
dslr = slr/y2d*dt;                       %slr/dt (m)

w = ws*d2s;                              %vertical exchange in
    days
dExt = zeros(length(n),1);   c0 = dExt;  %external exchange
delta = zeros(n);                        %horizontal exchange
    matrix
for j=1:nc0                              %assign external
    exchanges
    c0(cE0(j,1),1) = cE0(j,2);
    dExt(delta0(j,1),1) = delta0(j,2);
end
%
for j=1:nci                              %assign internal
    exchanges
```

```
60          delta(deltai(j,1),deltai(j,2)) = deltai(j,3);
61      end
62
63      switch model
64          case 1
65              model = 'WZB fortran';
66              asmita_fortran();
67          case {2,3}
68              asmita_kragtwijk();
69      end
70      vm = vm';   ve = ve';    vt = vt';          %transpose output
            arrays
71  %     plotVolumes(t,vm,ve,vt,model)             %plot results
72
73  %-nested function
    ------------------------------------------------------------------
74      function asmita_kragtwijk()
75          mu = -mu;                              %Kragtwijk uses
                opposite convention
76          delta = delta+delta';
77          D = -delta;
78          for j=1:n
79              D(j,j) = sum(delta(j,:))+dExt(j);
80          end
81          Amat = D*d2s;                          %horizontal exchange
                matrix per day
82          Amat = Amat+diag(w.*s);                %LHS matrix (D+W)
83          dExt = dExt*d2s;
84          %-----------------------------------------%solve concentration
                as per WZB fortran
85          if model==2
86              [L,U] = lu(Amat);                  %LU factorization of
                    dispersion matrix
87              vm = zeros(n,nt);
88              vm(:,1) = v;    [ve(:,1),vt(1,1),vt1(1,1),vt2(1,1)] =
                    mkve(h,s,v,alpha,beta,n);
89              for jt=2:nt+1
90                  vmjt = vm(:,jt-1);
91                  [vejt,vtjt,vt1jt,vt2jt] = mkve(h,s,vmjt,alpha,beta,n
                        ); %equilibrium volume
92                  ce = cE.*(vejt./vmjt).^(mu.*en);  %local equilibrium
                        concentration
93                  rhs = dExt.*c0+w.*s.*ce;          %rhs of
                        conservation equation
94                  c = U\(L\rhs);                    %solve A.x = b
                        where A=amat and b=rhs
95                                                    %note: no
                                                          different to c
```

```
                                                    = amat\rhs;
96              dvm = mu.*s.*dslr;                  %change in water
                    volume due to slr
97              vmjt = vmjt+w.*s.*mu.*(ce-c)*dt+dvm;
98              vmjt(vmjt<0) = 0;                   %trap negative
                    volumes
99              vm(:,jt) = vmjt;                    %moving volume
100             ve(:,jt) = vejt;                    %equilibrium
                    volume
101             vt(1,jt) = vtjt;                    %tidal prism
102             vt1(1,jt) = vt1jt;
103             vt2(1,jt) = vt2jt;
104         end
105         model = 'Kragtwijk using conc';
106     %-------------------------------------------%solve using B and
            d explicit solution
107     else
108         D = D*d2s;                              %horizontal exchange
                matrix per day
109         W = diag(w.*s);
110         vm(:,1) = v;    [ve(:,1),vt(1,1),vt1(1,1),vt2(1,1)] =
                mkve(h,s,v,alpha,beta,n);
111         for jt=2:nt+1
112             vmjt = vm(:,jt-1);
113             [vejt,vtjt,vt1jt,vt2jt] = mkve(h,s,vmjt,alpha,beta,n)
                    ; %equilibrium volume
114             gamma = (vejt./vmjt).^(mu.*en);     %local equilibrium
                    ratio
115             B = diag(cE.*mu)*W*(eye(n)-(D+W)\W);
116             if sum(W)==0    %used to test code - only change is
                    water level
117                 dd = w;
118             else
119                 dd = diag(cE.*mu)*W*((D+W)\dExt);
120             end
121             dvm = mu.*s.*dslr;                  %change in water
                    volume due to slr
122             vmjt = vmjt+(B*gamma-dd)*dt+dvm;    %Eq.17 and !8,
                    Kragtwijk etal, 2004
123             vmjt(vmjt<0) = 0;                   %trap negative
                    volumes
124             vm(:,jt) = vmjt;                    %moving volume
125             ve(:,jt) = vejt;                    %equilibrium
                    volume
126             vt(1,jt) = vtjt;                    %tidal prism
127             vt1(1,jt) = vt1jt;
128             vt2(1,jt) = vt2jt;
129         end
```

```
130             model = 'Kragtwijk using B and d';
131         end
132     end
133 %-nested function
    ------------------------------------------------------------------
134     function asmita_fortran()
135         %solve concentration using matrix convention as per WZB
                fortran
136         delta = delta+delta';
137         D = delta;
138         for j=1:n
139             D(j,j) = -sum(delta(j,:))-dExt(j);
140         end
141         Amat = D*d2s;                           %horizontal exchange
                matrix per day
142         Amat = Amat-diag(w.*s);                 %LHS matrix (D+W)
143         dExt = dExt*d2s;
144
145         [L,U] = lu(Amat);                       %LU factorization of
                dispersion matrix
146         vm = zeros(n,nt);
147         vm(:,1) = v;    [ve(:,1),vt(1,1),vt1(1,1),vt2(1,1)] = mkve(h,
                s,v,alpha,beta,n);
148         for jt=2:nt+1
149             vmjt = vm(:,jt-1);
150             [vejt,vtjt,vt1jt,vt2jt] = mkve(h,s,vmjt,alpha,beta, n);
                  %equilibrium volume
151             ce = cE.*(vmjt./vejt).^(mu.*en);    %local equilibrium
                  concentration
152             rhs = -dExt.*c0-w.*s.*ce;           %rhs of conservation
                  equation
153             c = U\(L\rhs);                      %solve A.x = b where A
                  =amat and b=rhs
154                                                 %note: no different to
                                                        c = amat\rhs;
155             dvm = mu.*s.*dslr;                  %change in water
                  volume due to slr
156             vmjt = vmjt+w.*s.*mu.*(c-ce)*dt-dvm;
157             vmjt(vmjt<0) = 0;                   %trap negative volumes
158             vm(:,jt) = vmjt;
159             ve(:,jt) = vejt;                    %equilibrium volume
160             vt(1,jt) = vtjt;                    %tidal prism
161             vt1(1,jt) = vt1jt;
162             vt2(1,jt) = vt2jt;
163         end
164     end
165 end
166 %%
```

```
167 function [ve,vt,vt1,vt2] = mkve(h,S,v,alpha,beta,n)
168     %define equilibrium volumes
169     sbasin1 = S(1)+S(5);          %plan area of subbasin (west) (flat
            + channel)
170     sbasin2 = S(2)+S(6);          %plan area of subbasin (mid) (flat
            + channel)
171     sbasin3 = S(3)+S(7);          %plan area of subbasin (east) (flat
            + channel)
172     vt1 = sbasin1*h-v(1);         %tidal prism of subbasin west
173     vt2 = sbasin2*h-v(2);         %tidal prism of subbasin mid
174     vt3 = sbasin3*h-v(3);         %tidal prism of subbasin east
175     vta = vt2+vt3+((S(4)+S(8))*h)-v(4);    %tidal prism of large
            subbasin east
176     vt = vt1+vta+(S(9)*h);                 %tidal prism of basin
177     ve = zeros(n,1);
178     for i = 1:n
179         if i == 1 | i == 5
180             ve(i) = alpha(i)*(vt1^beta(i));       %equilibrium
                volume west
181         elseif i == 2 | i == 6
182             ve(i) = alpha(i)*(vt2^beta(i));       %equilibrium
                volume mid
183         elseif i == 3 | i == 7
184             ve(i) = alpha(i)*(vt3^beta(i));       %equilibrium
                volume east
185         elseif i == 4
186             ve(i) = alpha(i)*(vta^beta(i));       %equilibrium
                volume acces flat
187         elseif i == 8
188             vet = alpha(i)*(vta^beta(i));         %channel
                equilibrium volume total eastern part
189             ve(i) = vet - ve(6) - ve(7);          %Acces channel
                equilibrium volume
190         elseif i == 9
191             vet2 = alpha(i)*(vt^beta(i));         %channel
                equilibrium volume total eastern part
192             ve(i) = vet2-ve(5)-ve(6)-ve(7)-ve(8); %Acces channel
                equilibrium volume
193         elseif i == 10
194             ve(i) = alpha(i)*(vt^beta(i));        %equilibrium
                volume delta
195         end
196     end
197 end
198 %%
```